Biosynthesis of Co_3O_4-ZnO Nanocomposite Material Using Waste Extract of Potato and Banana Fruits Peel for Antibacterial Application

By:

Reta Demissie

A Thesis Submitted to the Department of Applied Chemistry

School of Applied Natural Science

Presented for the Partial Fulfillment of the Requirements for the Degree of Master of Science in Applied Chemistry (Physical Stream)

Office of Graduate Studies

Adama Science and Technology University (ASTU)

October, 2020

Adama, Ethiopia

Biosynthesis of Co_3O_4-ZnO Nanocomposite Material Using waste Extract of Potato and Banana Fruit peel for Antibacterial Application

By: Reta Demissie

Major advisor: Fedlu Kedir (PhD)

Co-advisor: Gemechu Deressa (PhD)

A Thesis Submitted to the Applied Chemistry Department

School of Applied Natural Science

Presented for the Partial Fulfillment of the Requirements for the Degree of Master of Science in Applied Chemistry (Physical Stream)

Office of Graduate Studies

Adama Science and Technology University (ASTU)

October, 2020

Adama, Ethiopia

Adama Science and Technology University

School of Applied Natural Science
Applied Chemistry Department
Approval Sheet

This is to certify that the thesis prepared by Reta Demissie, entitled ‘‘Biosynthesis of Co_3O_4-ZnO Nanocomposite Material Using waste Extract of Potato and Banana Fruits Peel for Antibacterial Application” and submitted in the partial fulfillment of the requirements for Master of Science in applied Chemistry (Physical Chemistry) complies with the regulation of the university and meets the accepted standards with respect to originality and quality of the thesis work.

_____	_____	_____
Name of student	Signature	Date
_____	_____	_____
Advisor	signature	Date
_____	_____	_____
Co-advisor	signature	Date
_____	_____	_____
Internal Examiner	Signature	Date
_____	_____	_____
External Examiner	Signature	Date
_____	_____	_____
Chairperson	Signature	Date
_____	_____	_____
Department Head	Signature	Date
_____	_____	_____
School Dean	Signature	Date
_____	_____	_____
Postgraduate Dean	Signature	Date

DECLARATION

I hereby declare that the thesis entitled "Biosynthesis of Co_3O_4-ZnO Nanocomposite Material Using Waste Extract of Potato and Banana Fruits Peel for Antibacterial Application" has been carried out by me under the supervision of Dr. Fedlu Kedir and Dr.Gemechu Deressa, during the year 2020 as part of Master of Science Program in Physical Chemistry. I further declare that this work has not been submitted to any other Universities or institutions for the award of any degree. All quotations and their sources are specifically acknowledged by means of references.

Name: Reta Demissie

Signature _____

This M.Sc thesis has been submitted for examination with our approval as thesis advisors.

Advisor Name: Fedlu Kedir (PhD)

Signature _____

Co-Advisor Name: Gemechu Deressa (PhD)

Signature _____

Date of Submission _____

Table of Content

ACKNOWLEDGEMENTS

First I would like to thank the only almighty God, who provides health, strength and accurate insight into reality for his divine intervention during my research work. Although this thesis work ultimately represents my accomplishments, I have benefited significantly from multiple peoples that I would like to acknowledge. First and foremost, I am grateful to goes to my advisors: Dr. Fedlu Kedir and Dr. Gemechu Deressa for their excellent supervision and scientific input in this research work.

Again I would like to give the dearest and greatest thanks to Mr.Eneyew Tilahun from School of Applied Natural Science, department of Applied Chemistry program for his willingness to share his knowledge and experience about methods of synthesis of nanocomposite. I would like to express my sincere gratitude to all academic, technical and support staff of the Program of Applied Chemistry, Adama Science and Technology University for providing the necessary knowledge, assistance and facilities to conduct my research work. Next I want to thank my family who were big sources of inspirations throughout my academic career with their valuable moral support and advice.

LIST OF ABBREVIATIONS

B. subtilis	Bacillus subtilis
BCC	Body centered cubic
CBD	Chemical bath deposision
DNA	Deoxyribonucleic acid
DRS	Diffused reflectance spectroscopy
E.coli	Escherichia coli
EDX	Energy Dispersive x-ray spectroscopy
E_g	Bandgap energy
FCC	Face centered cubic
FTIR	Furrier transform infrared
GRAS	Generally recognized as safe
HCP	Hexagonal close packed
K.pneumonia	Klebsiella pneumoniae
MARSA	Methicillin resistant staphylococcus aureus
MIC	Minimum inhibitory concentration
NPs	Nanoparticles
PEN	Project on emerging nanotechnology
ROS	Reactive oxygen species
SEM	Scanning electron microscopy
S.aureus	Staphylococcus aureus
TB	Tuberculosis
UV-Vis	Ultra violet visible
XRD	X-ray Diffraction

LIST OF FIGURES

LIST OF TABLES

ABSTRACT

In this study we have synthesized Co_3O_4, ZnO NPs and Co_3O_4-ZnO nanocomposites through biological method using cobalt nitrate hexahydrate and zinc acetate dihydrate as a precursor material using waste extract of potato and banana fruits peel as a capping agent. The synthesized NPs and nanocomposites were characterized by thermogravimetric analysis (TGA/DTA), X-ray diffraction (XRD), scanning electron microscope (SEM), UV–vis diffuse reflectance spectroscopy (UV-DRS) and Fourier transform infrared (FTIR) spectroscopy. The optimized crystal size of the synthesized nanocomposite was found to be 13.54nm 30.02nm, and 9.39nm for biologically synthesized Co_3O_4 , ZnO nanoparticles and Co_3O_4-ZnO nanocomposite using extract of potato fruit peel, respectively. The crystal size of the synthesized nanocomposite using extract of banana fruit peel was also found to be 10.70, 12.79 and 9.52nm for biologically synthesized Co_3O_4, ZnO NPs and Co_3O_4-ZnO nanocomposite, respectively. The bandgap for synthesized Co_3O, ZnO NPs and Co_3 O_4-ZnO nanocomposite using peel of potato were 3.25, 3.08 and 3.33 eV, respectively. The bandgap for synthesized Co_3O_4,, ZnO NPs and Co_3O_4-ZnO nanocomposite using peel of banana were 3.60, 3.17 and3.56 eV, respectively. The XRD pattern with sharp peaks describes the crystalline and purity of Co_3O_4, ZnO NPs and Co_3O_4-ZnO nanocomposite. The morphology of Co_3O_4, ZnO nanoparticles and Co_3O_4-ZnO nanocomposite were studied by SEM analysis confirms spherical shape. FTIR spectrum discloses the interaction between the functional groups of the phytochemical in the fruit peel extract and the Co_3O_4, ZnO NPs and Co_3O_4-ZnO nanocomposite. Based on the results biologically synthesized Co_3O_4, ZnO nanoparticles and Co_3O_4-ZnO nanocomposite calcinated using extract of peel potato have potential antibacterial applications even in large concentration especially for gram negative bacteria compared to synthesized Co_3O_4, ZnO nanoparticles and Co_3O_4-ZnO nanocomposite in the presence of peel of banana.

Key word: *Co_3O_4, ZnO NPs and Co_3O_4-ZnO nanocomposite, Green synthesis, Sol-gel, Antibacterial activities*

1. INTRODUCTION

1.1. Background of the study

Nanotechnology deals with the production and design of utilizing nanoparticles. It emerges from the physical and chemical properties different from bulk and engineered techniques are being developed to search and plan single atoms and molecules for multiple applications in different field of scientific world. Nanoparticle (NP) is defined as a small object that behaves as a whole unit in terms of its properties. NPs are cluster of atoms having at least one dimension in the size range of 1–100 nm. They have unique optical, magnetic, catalytic and electrical properties. Thus have potential applications in various fields the physicochemical properties of NPs are different as compared to those of their bulk counterparts owing to the fact that surface area to volume ratio increases and quantum effects become dominant as the size decreases.

The increase in surface area to volume ratio alters the mechanical, catalytic and thermal properties of material [1]. The chemical methods include salt reduction method, reverse micelles, electrochemical method, Sol-gel method, gas-liquid interface, thermolysis, co-precipitation and decomposition on ultrasonic treatment. A vast array of biological resources available in nature including living plants, plant products, and plant extracts, Algae, fungi, yeast, bacteria and viruses could all be employed for synthesis of nanomaterial [2]. One of the global health and environmental concerns is the increasing antimicrobial resistance of many microorganisms against drugs because some pathogens which were curable in past now are becoming untreatable such as Methicillin-resistant staphylococcus aureus (MRSA) [3].

Humans have always war and struggle against the microorganisms that cause infection and disease to human health. To win this battle and to overcome this frightening situation of microbial resistance to antibiotics the search and discovery of alternative means against these microorganisms is only way forward to survive. Medicinal plants have a long history of use and their use is widespread in both developing and under developed countries [4]. There are many composition of banana skin like enzymes such as polyphenol oxidase, pectin as gelling agent and that the banana peel extract is used alone or combined with a cream or ointment, medicinal

benefits of the extract include relief of pain, swelling and itching [5, 6]. Additionally, Flavonoids, tannins, phlobatannins, alkaloids, glycosides and terpenoids were found to be present in the peels of genus (*Musa sapientum)*. These phytochemicals have been reported to exert multiple biological and pharmacological effects (antibacterial, antihypertensive, antidiabetic and anti-inflammatory activities). The presence of these bioactive substances in banana peels therefore suggests that the peels possess valuable medicinal potential yet to be explored. As the bioactive compounds contained in plants are majorly responsible for their medicinal properties [7].

Different studies have been done on the various parts of banana plant in which performed the inhibitory effect towards the food borne pathogens, hence banana plant should be considered to be a potential natural source of antimicrobial as well as antioxidant agent [8].The aim of this study was to assess the antimicrobial capacity of the aqueous extracts of fresh banana peels against different microbial isolates. The development of resistance among the microbial flora to the existing synthetic antimicrobial agents creates a very serious risk to public health [9-12]. Hence, alternative measures for the above problem should be addressed immediately, and consequently this state has led to a re-assessment of the therapeutic use of traditional medication, such as plants and plant-based products [13, 14]. Especially, the potato peels have various medicinal and nutritional values and they are the source of phenolic compounds, flavonoids, glycoalkaloids, and cell wall polysaccharides, vitamins and minerals like potassium[15, 16]. The glycoalkaloids present in Potato peels are toxic to microorganisms and these glycoalkaloids have beneficial properties, such as antipyretic, anti-inflammatory, and antimicrobial activities against pathogenic microbes[15].

Metals based nanoparticles and investigation of their antimicrobial activity could be one of such alternatives. Many studies are being done to check the structural and chemical effects of various metals nano-complexes to discover an alternative of the drugs which used against microorganisms. Cobalt oxide nanoparticles is among those materials which can be used for antimicrobial activity so the synthesis, characterization and antimicrobial activities of Cobalt based nanoparticles of great importance[17].The advantage of ZnO is their photocatalytic ability that can produce radical compounds. This material can be used as an antibacterial agent [18].

ZnO is also based nanomaterials have been intensively investigated because they are chemically stable and environmental friendly materials. In recent years, nanocomposites have been studied extensively due to their specific properties such as catalytic, optical, electrical, and magnetic properties, which are quite different from those for the bulk materials. Zinc oxide, well known wide band gap semiconductors compound, has important applications such as chemical sensors, varistors, UV emitters, catalysts, transparent high power electronics, surface acoustic wave devices, piezo-electric transducers, [19]. Various methods have been reported for the synthesis of ZnO nanoparticles such as sol-gel [20], Chemical Bath Deposition (CBD)[21], sonochemcial synthesis[22-24]. Many techniques could be applied in the sol-gel technology such as the changing of initial precursor, time of gel formation, type of catalyst, rate of solution formation, gel formation conditions and gel physical processing. Thus, the sol-gel process enables the formation of solid material through gelation from a solution [25].

1.2. Statement of the problem

Bacterial infectious diseases are serious health problem that has drawn the public attention in worldwide human health threat which extends to economic and social complications. Outbreaks infections of pathogenic strains, bacterial antibiotic-resistance, emergence of new bacterial mutations, lack of suitable vaccine is a reason why infection due to pathogen is increased [26]. In under developed countries hospital-associated infections are global health hazard to human particularly in children. Thus developing novel antibacterial agents against bacteria strains mostly major pathogens such as *Escherichia coli, staphylococcus aureus*, *Klebsiella pneumonia* and *Bacillus subtilis* has become greatest demand. These bacterial strains are selected as they are highly transmittable hence we can evaluate the potential antimicrobial activity of cobalt oxide and Zinc oxide NPs against these pathogenic bacteria. Different researches have done on the synthesis of Cobalt Oxide and Zinc oxide nanoparticles and cobalt oxide-zinc oxide nanocomposites for antibacterial applications. Furthermore, comparative study on Co_3O_4 and ZnO NPs synthesized by using cobalt nitrate hexahydrate and and Zinc nitrate tetrahydrate and their composites green method using peels of banana and potato extract as reducing and stabilizing agent against human pathogenic bacteria has not been reported yet.

1.3. Objectives of the Study

1.3.1. General Objective

The general objective of this project was to synthesize and characterize Co_3O_4, ZnO NPs and Co_3O_4-ZnO nanocomposite using sol-gel method from waste extract of potato and banana fruits peel and investigate their antibacterial applications.

1.3.2. Specific Objectives

- To synthesize Co_3O_4 NPs, ZnO NPs and Co_3O_4-ZnO nanocomposite using peel extract of banana and potato fruits
- To characterize the synthesized cobalt oxide, zinc oxide nanoparticles and Co_3O_4-ZnO nanocomposite using TGA-DTA, UV-Vis, FTIR, SEM, and XRD.
- To test antibacterial activities of Co_3O_4, ZnO and Co_3O_4-ZnO
- To compare antibacterial activity of biosynthesized cobalt oxide , zinc oxide NPs and Co_3O_4-ZnO nanocomposite against human pathogenic bacteria such as *Escherichia coli, staphylococcus aureus, Klebsiella pneumonia and Bacillus subtilis*

1.4. Significance of the Study

The study area was provided important information about the biologically synthesized cobalt oxide and zinc oxide nanoparticles and the composites of Co_3O_4-ZnO NPs characterization methods. This study area was also giving information about antibacterial activities of cobalt oxide and zinc oxide nanocomposite synthesized using sol-gel method. Also opens up further explorations on many fruits to be used for antibacterial applications.

1.5. Scope of the Study

Synthesis of cobalt oxide, zinc oxide nanoparticles and Co_3O_4-ZnO nanocomposite material using waste extract of potato and banana fruits peel as a reducing and capping agent by using sol-gel method.The synthesized Zinc oxide, Cobalt oxide and Cobalt oxide-Zinc oxide nanocomposites were characterized using TGA-DTA, UV-Vis spectrophotometer, FTIR Spectrophotometer, SEM, and XRD analysis. Finally, antibacterial activities of the biosynthesized nanomaterials were evaluated against human pathogenic bacterias such as *Escherichia coli, staphylococcus aureus, Klebsiella pneumonia and Bacillus subtilis* using sol-gel methods.

2. LITERATURE REVIEW

2.1. Nanoparticles

Nanotechnology refers to the production and usage of material with nanoscale dimension. It is a multidisciplinary scientific field undergoing explosive development and one of the most active research areas in modern material science. Because of Specific characteristics such as size distribution and morphology nanoparticles exhibit completely new or improved property. NPs have given rise to a busy area of research due to the wide variety of applications and novel properties such as biomedicine and with tunable electrical conductivity, thermal conductivity, superior rigidity, hard and erosion resistance. Nanomedicine is one of the main branches that affected tremendously by the nanoparticle applications that may be defined partially in the following areas: the monitoring, repair, construction and control of human biological systems at the molecular level, using engineered nanodevices and nanostructures. These nanomedicine has a vital role as bacteria are gaining resistance to traditionally used antibiotics at an alarming rate [27].The metallic oxide nanoparticles are most promising which is of much interest to researchers due to the growing microbial resistance against metal ions, antibiotics and the development of resistant strains[28].

2.2. Synthesis of Metal Oxide Nanoparticles

The methods for the synthesis of nanoparticles are physical, chemical and biological techniques. Physical synthetic methods such as inert gas condensation, high energy ball milling and ultrasonic shot peeling can be used to synthesize metallic nanoparticles [29]. Several methods including the commonly grinding process and pyrolysis can be used for the physical synthesis of metallic oxide nanoparticles. Disadvantage of physical methods is expensive and cumbersome for the large-scale production of nanoparticles[30]. A further drawback of physical approaches is enormous consumption of energy to maintain the high pressure and temperature used in the synthesis procedures. Chemical methods involve the reduction of chemicals, electrochemical procedures, micro emulsion, chemical co-precipitation and chemical vapor condensation.

Biological synthesis method of NPs which has the advantages of no toxicity, reproducibility in production easy scaling-up has become a new trend in nanoparticle production. Microorganisms and plants have been demonstrated as new resources with considerable potential for synthesizing nanoparticles[31]. In the case of biological method NPs synthesis using peel fruit waste extracts is the most adopted method because it is eco-friendly. The green method of production of nanoparticles is much safer to handle and easily available [32]. In addition, the synthesis of nanoparticles using fruits offers other advantages such as the utilization of safer solvents decreased use of dangerous reagents, milder response conditions, feasibility and their adaptability in use for medicinal, surgical and pharmaceutical applications. Also physical requirements for their synthesis including pressure, energy, temperature and constituent materials are trivial [33]. Many biomolecules in plants such as proteins, amino acids, carbohydrates, alkaloids, phenol compounds, reducing sugar and vitamins could be involved in bioreduction, formation and stabilization of metal nanoparticles. The reduction potential of ions and reducing capacity of plants which depend on the presence of polyphenols, enzymes and other chelating agent present in plants have critical effects on the amounts of nanoparticle production[34].

2.2.1. Cobalt Oxide Nanoparticles

Cobalt has been known with allotropic forms including face centered cubic (FCC), Hexagonal centered phase (HCP), epsilon and body centered cubic (BCC). The FCC structure is thermodynamically preferred at higher temperatures and the HCP structure is favored at lower temperatures. The FCC structure appears to be stable phase even below room temperature when the particle sizes are smaller than 20 nm [35]. There has been a considerable amount of research involving the preparation, structure and properties of magnetic cobalt nanoparticles in the past decade [36]. Cobalt nanoparticles coated with insulators have been prepared and studied for the applications in alternating current electrical and electronic devices[36]. Different crystalline structures provide some practical benefits. Symmetrically structured FCC cobalt provides higher saturation moment and lower magnetic anisotropy which is suitable for linear applications such as converter. On the other hand, asymmetric HCP-cobalt has been a basic element for high temperature permanent magnets and suitable for microwave applications such as in circulator. Cobalt nanoparticles often possesses mixed structures in which low energy stacking faults

introduce a combination of FCC and HCP character making the synthesis of single structured cobalt a challenging task. The potential applications of Cobalt oxide NPs in separation technology, catalysis, high-density magnetic recording and biomedicine are reviewed [37].

2.2.2. Zinc oxide nanoparticles

Zinc oxide has received a great attention since past times due to its various properties as: antibacterial, semiconducting properties, growth promoter[38], catalytic efficiency, chemical stability and strong adsorption ability. Because of these activities it has been used as an active ingredient for dermatological applications in creams, lotions and ointments and also ZnO which is widely used as food additive and food supplement [39]. ZnO is one of five zinc compounds that are listed as generally recognized as safe (GRAS) by the U.S. Food and Drug administration [40]. Either two antimicrobial mechanisms of ZnO are supposed. These are Hydrogen peroxide, which is generated from the surface of zinc oxide, can penetrate through the cell membrane, produce some type of injury, and inhibit the growth of the cells and the affinity between zinc oxide and bacterial cells is an important factor for antibacterial activity[38].

In addition zinc oxide is an interesting semiconductor material this is seen through its application on solar cells, gas sensors, ceramics, and varistors [41]. In nanoscience, ZnO nanoparticles show a significant growth inhibition under normal laboratory lighting conditions and in the same time they have selective toxicity and are regarded as a safe reagent to humans and animals, this action can be understood because ZnO inhibiting the adhesion and internalization of bacteria and so ZnO can protect against intestinal diseases caused by *E. coli* [42], and proved through the scanning electron microscopy (SEM), the morphological changes of *E. coli* treated with zinc oxide nanoparticles, which showed that ZnO nanoparticles could damage the membrane of this bacteria and so led to the leakage of cytosolic components and finally killed the bacterial cell. ZnO appeared that it has a significant antibacterial activity against a wide range of bacterial species and in particular against *S. aureus* [27]. In addition, another feature that made ZnO nanoparticles compete other metal oxide nanoparticles is its antibacterial activity against a broad range of bacteria: gram positive and gram negative [42].

2.3. Chemical Synthesis of Cobalt Oxide Nanoparticles

The transition metal oxides have greatly attracted wide range of application in durable solar absorber lithium-ion battery. As transition metal groups cobalt oxide Co_3O_4 NPs is one of the most important materials because of its fascinating properties and thermal stability. Co_3O_4 NPs show good conductivity due to the existence of Co^{3+} [43]. Cobalt nanocrystals display a wealth of size-dependent structural magnetic, electronic and catalytic properties. The cobalt structure of p-type semiconducting materials with chemical stability at high mechanical strength and the direct optical band gaps of Co_3O_4 nanoparticles were about 1.48 and 2.19 eV [44].

2.4. Chemical synthesis of Zinc Oxide nanoparticle

ZnO is technologically an important material for its wide range of optical and electrical properties; also it is crystal with a typical wide band gap n-type direct band gap semiconductor material with lower resistivity and higher light trapping properties wide band gap (3.37eV)[45]. Such properties make semiconducting nanostructures suitable for several kinds of applications, from antireflecting coatings[46] to bioelectronics[47] and light emitting devices[48] antibacterial treatment[46], UV light emitters[49] photocatalyst[50] and as an additive in many industrial products. It is also used in the fabrication of solar cells[46], gas sensors, luminescent materials, transparent conductor. Inorganic nanoparticles are important materials for applications in medicine, such as biosensing, cell imaging, drug delivery, cancer therapy [50, 51].

According to the Project on Emerging Nanotechnologies (PEN), ZnO occupies fifth rank among the most prevalent nanomaterials in consumer products. ZnO can have two different crystal structures (zinc blende and wurtzite), both of which have the same band gap energy (3.3 eV) and the direct band structure. Localized trap states inside the band gap were studies[46] in detail to recognize the sub-band gap energy levels. Moderate reaction conditions and convenient synthetic manipulation have rendered chemical methods an attractive option for accessing ZnO nanoparticles. The method also provides better control of chemical and morphological characteristics. The chemical method involves the use of toxic chemicals which can prove to be hazardous for the environment and the person handling it. These methods may result in toxic and

harsh products which may pose biological risks to the environment; due to high surface charge and high surface area of nanoparticles, harsh chemicals may remain adsorbed onto nanoparticles. Releasing these chemicals into the environment may cause adverse effects on organisms including microorganisms, plants, invertebrates, and vertebrates including humans at various trophic levels[2]. These drawbacks have led to the emergence of green synthesis methods based on the use of environmentally friendly and biocompatible materials such as plants and microorganisms.

2.5. Biosynthesis of Cobalt Oxide Nanoparticles

Extract from bio-organism may act both as reducing and capping agent in nanoparticles synthesis. The reduction of metals ions by bimolecular found in these extracts such as protein, polysaccharide, vitamin and amino acid is environmentally save. Biological methods are regarded as safe, cost effective, sustainable and environmental friendly processes for the synthesis of nanoparticles. Biological synthesis of nanoparticles is gaining importance due to its eco friendliness and simplicity [52]. The use of plant materials in the synthesis of cobalt oxide nanoparticles has been reported by other researchers [53].

2.6. Biosynthesis of Zinc Oxide Nanoparticles

Biosynthesis of nanoparticles is an approach of synthesizing nanoparticles using microorganisms and plants having biomedical applications. Biosynthesis provides more advantages over physical and chemical methods because it is very cost effective, non-toxic, uses safe reagents during the process [54] and eco-friendly technique due to use of extracts of plant (leaves, flower, seed and peels), bacteria, fungi and enzymes, as the reducing and stabilizing agents for synthesis of nanoparticles instead of large quantity of chemicals[54]. This method does not require high temperature, high pressure, costly equipment and hazardous chemicals. The three main aspects in the preparation of nanoparticles that should be evaluated from a green chemistry perspective are the choice of the solvent medium used for the synthesis, the choice of an environmentally favorable reducing agent and the choice of a non-toxic material for the stabilization of the nanoparticles. The progress of efficient green synthesis utilizing natural reducing, capping and

stabilizing agents without the use of toxic, expensive chemicals and high energy consumption have attracted researchers towards biological methods[55].The biological method of synthesis of ZnO nanoparticles is gaining importance due to its simplicity, eco-friendliness and extensive antimicrobial activity.

2.7. Biosynthesis of Co_3O_4-ZnO Nanocomposite

Green synthesis of metal oxide nanocomposite has received special attention due to a cheaper and environmentally friendly method. It can refer to the formation of nanoparticle structures which capped by organic materials from living organisms or plants [56]. An important use of nanoparticles and nanotubes is in composites, materials that combine one or more separate components and which are designed to exhibit overall the best properties of each component. This multi-functionality applies not only to mechanical properties, but extends to optical, electrical and magnetic one nanocomposites of zinc, cobalt, nickel, silver and iron are being studied extensively as potential antimicrobial agents owing to the beneficial synergistic effects of their components and to discover their enigmatic role in medical nanotechnology [57]. Several methods are used for metal oxide nanocomposite synthesis such as hydrothermal[58], electrochemistry [59], wet chemical [60], microwave method [61] coprecipitation, sol–gel, wet impregnation, and thermal decomposition [62-65]. Moreover, Co_3O_4-ZnO nanocomposite has been known as a good photocatalyst that can work in the visible light area. Here in, we investigate a simple and an environmentally friendly method to synthesise Co_3O_4-ZnO nanocomposite.

2.8. Antibacterial Activity of Metallic Oxide NPs

Metal based nanoparticles represent an alternative for biomedical treatments mainly in the fabrication of biomedical devices with antimicrobial coatings. A high antimicrobial activity of nanoparticles depends on the particle size that allows greater surface contact and a direct interaction with the membranes microorganisms. Nanoparticles smaller than 10nm highly interact with bacteria and produce electronic effects which improve the reactivity of nanoparticles. Thus it is proven that the bactericidal effects of nanoparticles are size dependent

[66]. The cell membranes of the microorganisms interact with the medium so metal oxide NPs have some interactions to release metal ions that interfere with the processes of the deoxyribonucleic acid (DNA) replication, cell membrane formation and cell division[67]. Several studies propose that nanoparticles attach to the surface of cell membrane disturbing the permeability and respiration function of the cell.

The damage to the cell may be caused by the interaction of nanoparticles with sulfur or phosphorus containing bio molecules in the cell such as DNA. Therefore sulfur containing proteins in the membrane or inside cells and phosphorus containing molecule like DNA are likely to be preferential sites for binding NPs. The smaller nanoparticles have more antibacterial activity that provides more surface exposure to the bacterial membrane[68]. In addition these nano sized particles penetrate through cell membrane easier interacting with intracellular materials and finally resulting in cell destruction in the process of multiplication[69]. Documented that the nanoparticles induce oxidative stress to bacteria and induce reactive oxygen species (ROS) thus antibacterial activity could be explained based on ROS such as hydrogen peroxide (H_2O_2) Hydroxyl radicals (OH^-) and singlet oxygen (O^-). It is believed that microorganisms carry a negative charge while metal oxides carry a positive charge. This creates an electromagnetic attraction between the microbe and treated surface[70].

2.9. Antibacterial Activity of Cobalt Oxide NPs

Currently several antimicrobial drug are used to kill microbe or prevent the growth of microbe. However with the worldwide use and abuse of the most commonly used antibacterial drugs microorganisms especially bacteria are becoming resistant to more and more antimicrobial agents for example bacteria strains known to be cause tuberculosis (TB) are found to be resistant to previous effective antibacterial treatment. *E. coli* is found to be intrinsically resistant to therapeutic level of penicillin. The first beta lactam introduced into clinical practice because of its outer membrane barrier. *E.coli* is also resistant to several different classes of antibiotics with distinct mechanism of action[71]. There are many advantages among using metal NPs as antimicrobial agents due to their stability, Robustness and self-life**.** Nano sized cobalt oxide NPs have shown to possess antibacterial activities and several studies reported that they can be used

as bactericides for water disinfection. The antibacterial activities of cobalt oxides NPs against *E.coli, S. aureus, Kpneumonia and B. subtilis* were examined. The performance of Cobalt oxide NPs for antibacterial activities prepared by biological and chemical methods to wards microbial have not been studied well. Therefore, it is important to study comparison of biologically and chemically synthesized cobalt oxide NPs for antibacterial applications [72].

2.10. Antibacterial Activity of Zinc Oxide Nanoparticles

In nanoscience, ZnO nanoparticles show a significant growth inhibition under normal laboratory lighting conditions and in the same time they have selective toxicity and are regarded as a safe reagent to humans and animals, this action can be understood because ZnO inhibiting the adhesion and internalization of bacteria and so ZnO can protect against intestinal diseases caused by *E. coli* [42]. The morphological changes of *E. coli* treated with zinc oxide, which showed that ZnO nanoparticles could damage the membrane of these bacteria and so led to the leakage of cytosolic components and finally killed the bacterial cell [38]. Zinc oxide nanoparticles have stronger antibacterial activity due to largely increased surface or enhanced the affinity[38]. ZnO appeared that it has a significant antibacterial activity against a wide range of bacterial species and in particular against *S. aureus* [27].

The antimicrobial property of ZnO nanoparticles also were analysed with *K.pneumonia and B. subtilis* using agar well diffusion. It has been suggested that the mechanism of the antibacterial activity of ZnO NPs is based on its ability to induce oxidative stress [73]. The Zn^{+} ions released interact with the thiol group of the bacterial respiratory enzymes, increasing the production of reactive oxygen species (ROS) and causing oxidative stress in the bacterial cell. This oxidative stress damages the bacterial membranes, DNA, and mitochondria, resulting in the death of the bacteria [74-76] . In addition, another feature that made ZnO nanoparticles compete other metal oxide nanoparticles is its antibacterial activity against a broad range of bacteria: gram positive and gram negative[42].

2.11. Antibacterial activity of Co_3O_4-ZnO nanocomposite

In the present work, we report the detailed investigations of in vitro antibacterial activities of α-Co_3O_4-ZnO nanocomposite against four pathogenic bacteria *B. subtilis*, *S. aureus*, *E.coli* and *K. pneumonia*. The nanocomposites were synthesized using cost-effective wet-chemical approach and further characterized to study the structural, morphological, optical and magnetic properties. Hence this study was carried out to mainly investigate the antibacterial properties of Co_3O_4-ZnO nanocomposite. The simultaneous use of different mechanisms results in a situation where it was very unlikely for the bacterial cell to develop resistance to these nanoparticles because to do so, the bacteria have to go through multiple mutations simultaneously in a single cell which is a very rare event and almost impossible. Additionally, cytotoxicity of the prepared composite samples was evaluated and the prepared samples were found non-toxic to human cell line.

2.12. Antibacterial strains

Staphylococci among the pathogenic bacterial strains are the common bacteria that cause a wide varity of infections and diseases especially hurt skin and mucus membranes. On the other hand, *E. coli* enteric bacteria that are currently more implicated in many digestive tract and urogenital infections with the high incidence of septicemia cases.

2.12.1. Staphylococcus aureus

Staphylococci are gram positive bacteria that are characterized by individual cocci that appear to be divided into more than one plane to form grape like cluster that are none motile and non-spore forming [77, 78]. S. aureus are facultative anaerobes and grow by aerobic respiration or by fermentation pathogenic *S. aureus* is a member of the genus staphylococci which is named aureus due to the golden color appearance as it grown on solid media.

2.12.2. Escherichia coli

Escherichia coli is gram negative bacteria which is known to be both natural flora of humans and more over some important pathogens that considered a significant cause of morbidity and

mortality worldwide. It characterized by a non-spore forming, motile, rode shaped bacteria that ferment lactose[79]. *E.coli* strains are comparatively easy to grow under both aerobic and anaerobic conditions[79]. Some of *E. coli* isolates are considered part of beneficial normal flora of the intestine but some strains appeared to acquire pathogenicity mechanisms to cause disease in human such as urinary tract infection and sepsis or meningitis.

2.12.3. Bacillus Subtilis

Bacillus subtilis is a gram positive bacterium characterized by aerobic, spore-forming, rod-shaped bacteria that are motile by peritrichous flagella. These bacteria are extensively spread throughout the environment, particularly in soil, air, and decomposing plant residue[77]**.** The distinction of these bacteria are their capability of producing endospores that are highly resistant to unfavorable environmental conditions and that also have capacity to grow over a wide range of temperatures including that of the human body.

2.12.4. Klebsiella Pneumoniae

This organism accounts for about one-third of all Gram-negative infections such as urinary tract infections, cystitis, pneumonia, surgical wound infections, endocarditis and septicemia. It also causes necrotizing pneumonia, pyogenic liver abscesses and endogenous endophthalmitis [80].
High mortality rates, extended hospitalization, coupled with high cost are often associated with infections caused by this organism [81].Designed to determine the antibiotic-resistant profiles of *Klebsiella pneumonia* as a nosocomial pathogen and focuses on some differences between classical and non-classical subtypes, antimicrobial resistance-mediated genes, some virulent factors of this organism, and some epidemiological risk factors through a systematic review and meta-analysis.

3. EXPEREMENTAL SECTION

3.1. Materials

In this research, zinc (II) acetate dihydrate [Zn $(CH_3\ COO)_2 \cdot 2H_2O$] and Cobalt nitrate hexa hydrated [Co $(NO_3)_2.6H_2O$] were used as precursors for the synthesis of ZnO and Co_3O_4 NPs, respectively. Sodium hydroxide (NaOH) and ethanol were used as precipitating agent and for washing purpose, respectively. Distilled water was used as the synthesis medium. All chemical reagents were purchased from market and are analytical grades.

3.2. Collection of the peels of banana and potato fruits waste

The collected waste extract of potato and banana fruits peel were thoroughly washed with distilled water to remove impurities such as dust and other particulates followed by drying under shadow with room temperature to remove residual moisture. The dried waste extract of potato and banana fruit peels were grinded using plant grinding machine and then were packed within a plastic bottle for further use. To prepare the extract of the banana and potata peel, 20 gram of each were taken and dissolved in to 250 mL of distilled water in 500 mL Erlenmeyer flasks. The Erlenmeyer flask containing the components were placed on to a hot plate with magnetic stirrer, and allowed to boil at 60℃ for about 30 minutes.The extracted solutions of the banana peel and potato peel were kept under refrigerator at 4^oC for biosynthesis of Co_3O_4 Nps, ZnO NPs and Co_3O_4-ZnO nanocomposite. The filtrate extract was used as reducing and capping agent for the biosynthesis of Co_3O_4-ZnO nanocomposite[82].

3.3. Synthesis of Cobalt Oxide NPs

Cobalt nitrate hexahydrate $Co(No_3)_2.6H_2O$) was dissolved in the waste extract of potato and banana fruits peel. To optimize the proportion of cobalt nitrate hexahydrate and waste extract of potato and banana fruits peel during synthesis of Co_3O_4 nanoparticles 1:1,1:2 and 2:1 ratios of waste extract of potato/ banana fruits peel and precursor salt were used. Then three different samples were prepared by taking different volume ratios of precursor salt solution and waste fruits peel extract. In 2:1 ratio: 40 mL of 0.75 M cobalt nitrate hexahydrate and 20 mL of waste

extract of banana and potato fruits peel. In 1:2 ratios: 20 mL of 0.75 M cobalt nitrate hexahydrate and 40 mL of waste extract of banana and potato fruits peel, and in 1:1 ratio: 30 mL of 0.75M cobalt nitrate hexahydrate and 30 mL of waste extract of banana and potato fruits peel. For the biosynthesis of Co_3O_4 nanoparticles within 2:1, 1:2 and 1:1 ratio approximately (40:20), (20:40) and (30:30) of volume ratios were taken, respectively and this was done using 0.75 M of cobalt nitrate hexahydrate in a separate Erlenmeyer flask.

In each case the Erlenmeyer flask containing the three components were placed on to a plate with magnetic stirrer without applying of heat. In each of the different ratios a small sized magnetic stirrer was placed in to the Erlenmeyer flask containing the extract and the precursor solution and the resulting solution was allowed to stir for about 2 hours and then its pH value was measured using a pH meter and then 10 ml of 1M sodium hydroxide solution was added in to each of the individual ratio as a precipitating agent. After addition of a small drop of sodium hydroxide solution for each of the individual ratios, the resulting solution was stirred for 15 minutes to maintain uniform distribution of the added base followed by centrifugation at 10,000 rpm for 15min.The formed dark green color precipitate for each of the individual ratio was washed with distilled water and ethanol several times. The formed Co_3O_4 NPs were collected using a crucible ceramic dish and placed in to a drying oven for 5 hours at 80℃ [83] and then allowed to cool. The particles were stored in an air tight container [84].

3.4. Synthesis of Zinc Oxide NPs

The measured amount of the precursor salt of zinc acetate dihydrate ($Zn(CH_3COO)_2.2H_2O$) was mixed with the waste extract of potato and banana fruits peel. For the biosynthesis of ZnO nanoparticles within 2:1, 1:2 and 1:1 ratio approximately (40:20), (20:40)and (30:30) mL were taken, respectively and this was done using 0.75 M of zinc acetate dihydrate in a separate Erlenmeyer flask. In each of the different ratios a small sized magnetic stirrer was placed in to the Erlenmeyer flask containing the waste extract of potato and banana fruits peel and the precursor solution and the resulting solution was allowed to stir for about 2 hours and then its pH value was measured using a pH meter and then 10 ml of 1 M sodium hydroxide solution was added in dropwise manner for each of the individual ratio as a precipitating agent[85]. The

mixture was kept for 48 hours to form a pale white colored precipitate and washed with distilled water and ethanol several times during centrifugation. Then, the gel was dried in an oven at 100 °C to constant weight and calcined at 400 °C for 4 hours to obtain the ZnO nanoparticles[86].

3.5. Synthesis of Co_3O_4-ZnO Nanocomposite

Co_3O_4-ZnO nanocomposite was prepared by one- pot green synthesis method using the reaction of $Zn(CH_3COO)_2.2H_2O$ and $Co(NO_3)_2.6H_2O$ solutions with the waste extract of potato and banana fruits peel in Erlenmeyer flask. To examine the effect of proportion of Co_3O_4-ZnO nanocomposite and waste extract of potato and banana fruits peel on the size and crystallite of Co_3O_4-ZnO nanocomposite, 1:1, 1:2 and 2:1 ratios of waste extract of potato and banana fruits peel and precursor salt were used during the biosynthesis process. The mixture was stirred with magnetic stirrer to achieve homogeneity, and 10 ml of 1M NaOH was added to the solution in dropwise manner under stirring for about 2 hour, the process was also be followed by centrifugation to obtain brown colored precipitation[87]. The obtained gel was dried on oven at 80°C[88] and calcined at 400^o C for 4 hours to produce the Co_3O_4-ZnO nanocomposite.

3.6. Characterization of Co_3O_4 and ZnO NPs using TGA –DTA

Thermal gravimetric analysis (TGA) of the biosynthesized NPs was carried out using a simultaneous differential thermal analysis DTA-TGA (DTG-60H, Shimadzu Co., Japan) and was used to determine the calcination temperature. The synthesis of these nanomaterials with controlled size and shape was still a major challenge and large scale synthesis of phase pure Co_3O_4 and ZnO nanoparticles at relatively low temperatures, using readily available, environmentally benign and cost-effective precursors was a synthetic challenge. Thus, the preparation of cobalt oxide and zinc oxide nanoparticles in the presence of extract of peels of potato and banana by thermal decomposition of cobalt and zinc complexes becomes increasingly important mainly due to its cost-effectiveness, careful choice of precursors and calcination conditions, easy control of synthesis conditions, particle size, crystal structure, and purity. For example, the synthesis of metal oxide nanoparticles by the thermal decomposition of organometallic compounds or metal complexes has been reported [89-92].

3.7. Characterization of Co_3O_4, ZnO and Co_3O_4-ZnO Using XRD Analysis

The crystalline structure and average crystalline size of the synthesized Co_3O_4, ZnO nanoparticles and Co_3O_4-ZnO nanocomposites were investigated using an X-ray diffractometer at Adama Science and Technology University department of Material Engineering. XRD spectrum was recorded from 10^o to 80^o with 2θ angles using CuKα (λ =1.54056 A^o) radiation operated at 40 kV and 30 mA.

Debye Scherrer"s equation indicated in equation 1, was used to estimate the average crystallite size for powder samples of the synthesized nanoparticles[93].

$$D = \frac{0.94\lambda}{\beta \cos\theta} \quad \text{.....} \quad (1)$$

Where D is the crystallite size, λ = 1.54 A^o is the X - ray source wavelength, β is the full width at half maximum intensity of the peak position and θ is the peak position.

3.8. SEM Analysis of Co_3O_4 NPs, ZnO NPs and Co_3O_4-ZnO Nanocomposite

From biologically synthesized nanoparticles of Co_3O_4, ZnO and Co_3O_4-ZnO, small amount was taken and characterized by scanning electron microscopy-energy dispersive x-ray spectroscopy. SEM was provided information about the synthesized sample including morphology, chemical composition and crystalline structure. It is also provided detail high resolution images of the sample focused electron beam across the surface and detecting secondary or backscattered electron signal[94].

3.9. Characterization of Co_3O_4, ZnO and Co_3O_4-ZnO Nanocomposite using UV-Vis Spectrophotometer

The UV Vis absorption spectra of the biosynthesized Cobalt oxide, Zinc oxide nanoparticles and Co_3O_4-ZnO nanocomposites were recorded by using JASCO V-670 UV-Vis spectroscopy equipped with a diffuse reflectance attachment for powder samples from the waste extract of potato and banana fruit peels were confirmed by using a wavelength scan between 200 nm and

800 nm. Their characterization techniques were also giving information about bandgap energy of the biosynthesized Co_3O_4 ZnO, nanoparticles and Co_3O_4-ZnO nanocomposite.Their characterization techniques of the band gap energy of ZnO, Co_3O_4 NPs and Co_3O_4-ZnO nanocomposites were calculated based on the Tauc equation relation.

$$\alpha hv = B(hv - E_g)^n \quad \text{.....(2)}$$

Where h is the Planck constant, ν is the frequency of the vibration, α is the absorption coefficient, B is the constant, E_g is the band gap of the semiconductor, and n is a constant depends on the type of transition, which is 1/2 for a direct transition or 2 for an indirect transition of the synthesized Co_3O_4 and ZnO nanoparticles [95].

3.10. FT-IR Analysis of Co_3O_4, ZnO NPs and Co_3O_4-ZnO Nanocomposites

This characterization technique was carried out on biologically synthesized cobalt oxide, zinc oxide nanoparticles and Co_3O_4-ZnO nanocomposite to confirm the role of extracts used during synthesis. FTIR measurements of the samples were performed at wave number range between uses of 4000-400 cm^{-1}.The green synthesized cobalt oxide NPs, zinc oxide NPs and Co_3O_4-ZnO nanocomposite were analyzed using Fourier Transform Infrared (FTIR) Spectrometer. Also to determine the functional group in which bimolecular present in the peels extract[96].

3.11. Preparation of Inoculums for Antibacterial Test

Nutrient broth (1.5 g within 100 mL of distilled water) was prepared in 4 different conical flasks and then sterilized. The pure prepared cultures were subcultured. In the first conical flask clinically isolated strain of *staphylococcus aureus* and in the second conical flask clinically isolated strain of *Escherichia coli* was inoculated. In the third conical flask, clinically isolated strain of *Klebsiella pneumonia* and in the final conical flask clinically isolated strain of *Bacillus subtilis* was added. These different bacterial cultures were inoculated in nutrient broth and were allowed to keep on rotary shaker at 35°C± 2°C for about 24 hours at 160 rpm.

3.12. Inoculation of the Test Plates

Nutrient agar was prepared by taking 6 g nutrient agar and 0.8 g Agar-Agar followed by dissolving them within a given 100 mL of deionized water. After that, the prepared nutrient agar was sterilized. The prepared agar suspension was used to inoculate plates by dipping a sterile cotton wool swab into the suspension. Before applying the antibiotic disks, the plates were allowed to dry completely. The nutrient agar medium was used to cultivate both gram positive and gram-negative bacteria strains. The plates was incubated at 37^0C for about 16 - 18 hrs in an incubator for bacteria and was checked for the zone of inhibition[97].

3.13. Disc Diffusion Method

Antibacterial tests were carried out at Adama Science and Technology University at Biology department by the disc diffusion method using the suspension of bacteria spread on nutrient agar. The antibacterial activity of biosynthesized Co_3O_4, NPs ZnO NPs and Co_3O_4-ZnO nanocomposites (1:1, 1:2, and 2:1 ratios) and that of extract of peels of potato and banana were investigated using the disc diffusion method using Müller-Hinton broth agar against both Gram-positive bacteria strains of *Staphylococcus aureus* and *Bacillus subtilis* and Gram-negative bacteria strains of *Escherichia coli* and *Klebsiella pneumonia*. Four bacterial cultures from each bacterial strains were maintained on nutrient Müller-Hinton agar at 37°C, and the cultures were kept in appropriate media slants and stored at 4°C (to allow diffusion) until used. The plates were incubated at 37°C for 16-18 h in an incubator and were shaken gently to allow evenly mixing of bacteria cells and agar. Then, 50mg, 75mg and100mg from each of the three ratios of Co_3O_4, NPs ZnO NPs and Co_3O_4-ZnO nanocomposites (1:1, 1:2, and 2:1 ratios) were taken and dissolved within 1mL of DMSO to obtain 50mg/ml, 75mg/ml and100mg/ml. From each different ratio, the inoculated plates were incubated at 37°C for about 24 hours. In antibacterial testing against each strain, triplicate measurements were collected and the averages of the triplicates were used in reporting the result. Then antimicrobial activity was evaluated by measuring the zone of inhibition against the test bacteria *staphylococcus aureus*, *Escherichia coli, Klebsiella pneumonia and Bacillus subtilis* diameters of zones of inhibition of the control strain and test was measured using a ruler[98].

4. RESULTS AND DISCUSSION

In this study cobalt oxide, zinc oxide nanoparticles and Co_3O_4-ZnO nanocomposite were synthesized by green method using extract of peel of potato and banana. The synthesized nanocomposites were characterized using TGA-DTA, XRD, SEM, UV -Vis DRS and FTIR spectroscopy and their antibacterial activity were measured and the zones of inhibition from diffrent NPs were compared. The antibacterial activities of synthesized nanoparticles were investigated using both gram positive and gram negative bacterial strains.

4.1. Thermal Gravimetric-Differential Thermal Analysis (TGA-DTA).

The processes performed during the heating can be recorded by the TG and DTA curves in Figure 1 (A and C). Regarding the data of the weight losses, they may appear already after a heating at 80 ^{0}C in some samples. Weight loss again continued up to 346°C associated with a strong exothermic peak in the DTA curve, which can be observed in the samples with organic content due to the combustion of organic molecules. Therefore, heating at 346^{0}C is necessary to obtain cobalt oxide (Co_3O_4) from precipitates. However, Co_3O_4, as a result of thermal analysis, 400°C was used as calcination temperature during this work.

Figure 1(B and D) also shows the TG/DTA curves of ZnO samples prepared. The DTA curve shows an endothermic peak at 80 °C which also reflects the weight loss in the sample. It reflects a strong exothermic peak at 332 °C due to crystallization of ZnO in the DTA curve. The mass of the sample reaches an approximately constant value above 495 °C. Another weight loss observed in the temperature interval 482–785 °C formed due to decomposition of acetate ions[99].

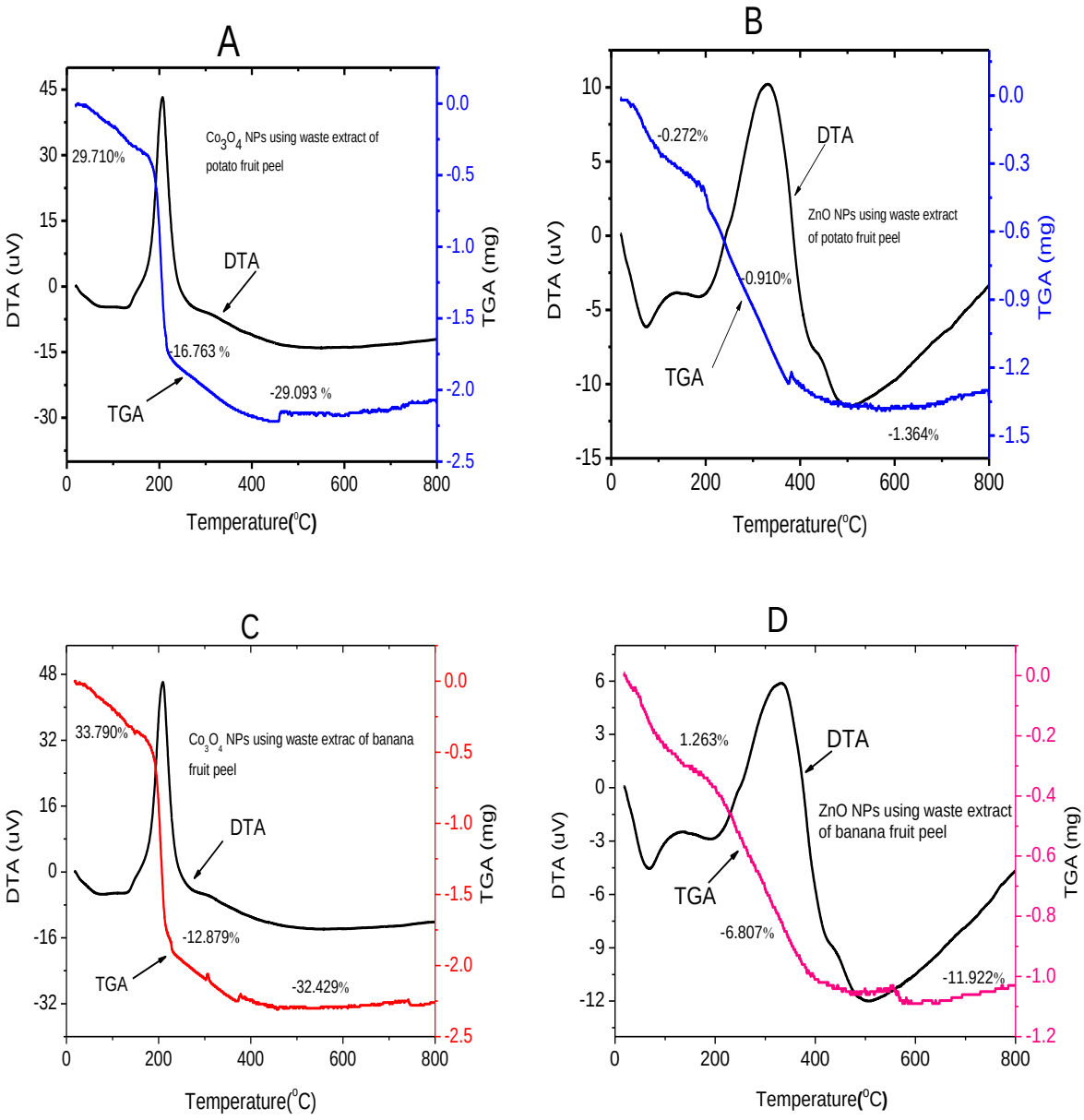

Figure 1. TGA-DTA analysis of as-synthesized cobalt oxide and zinc oxide NPs prepared from cobalt nitrate hexahydrate and zinc acetate dihdrate using extract of potato (A and B) and banana(C and D) fruits peels, respectively in a 1:1 ratio.

4.2. XRD Analysis

Figure 2 shows XRD patterns of Co_3O_4 NPs, ZnO NPs and Co_3O_4-ZnO nanocomposite biosynthesized from cobalt nitrate hexahydrate precursor, zinc acetate dihydrate and their composites and waste extract of potato fruit peels with in three different volume ratios. Cobalt oxide and zinc oxide nanoparticles formation and their composite were analyzed by x-ray diffraction. The XRD of Co_3O_4 NPs had some peaks appeared at 2θ values 18.8245, 30.9880, 36.8760, 44.8956, 59.3249, 65.7495 while ZnO NPs appeared at 2θ values 31.9207, 34.5528, 36.3926, 47.8407, 56.8994 and 62.7385, respectively. Miller indices of Co_3O_4 crystallite structures were (111), (220), (222), (400), (400), (511), and (440) while that of ZnO were (100), (002), (101), (102), (110), and (103).

The formation of biosynthesized Co_3O_4-ZnO nanocomposite was also confirmed by X-ray diffraction measurements and their peaks observed at 2θ values of 32.0613, 34.5954, 36.3394, 47.5638, 56.9250, 63.0664, 68.0153 and 69.4910 along with their corresponding miller indices values of (100), (002), (101), (102), (110), (103), (112), and (201), respectively. The intensity of diffraction peak of green synthesized Co_3O_4 nanoparticles is less with slight broadening when compared to the intensity of ZnO nanoparticles and Co_3O_4-ZnO nanocomposite. Those results reveals that the biosynthesized NPs have possessed good crystallinity in nature and also diffraction peaks related to impurities were not observed in the XRD pattern confirming the high purity of the biosynthesized nanomaterials.

The average crystalline size for the different kinds of Co_3O_4, ZnO NPs and Co_3O_4-ZnO nanocomposites were estimated as (18.8, 13.5, 19.45), (35.8, 30.0, 30.4), and (35.9, 9.4, 24.4), respectively from the given ratios of 1:1, 1:2 and 2:1 ratios. Thus the broadening of XRD peak of green synthesized nanocomposite observed in our study confirms the size reduction.

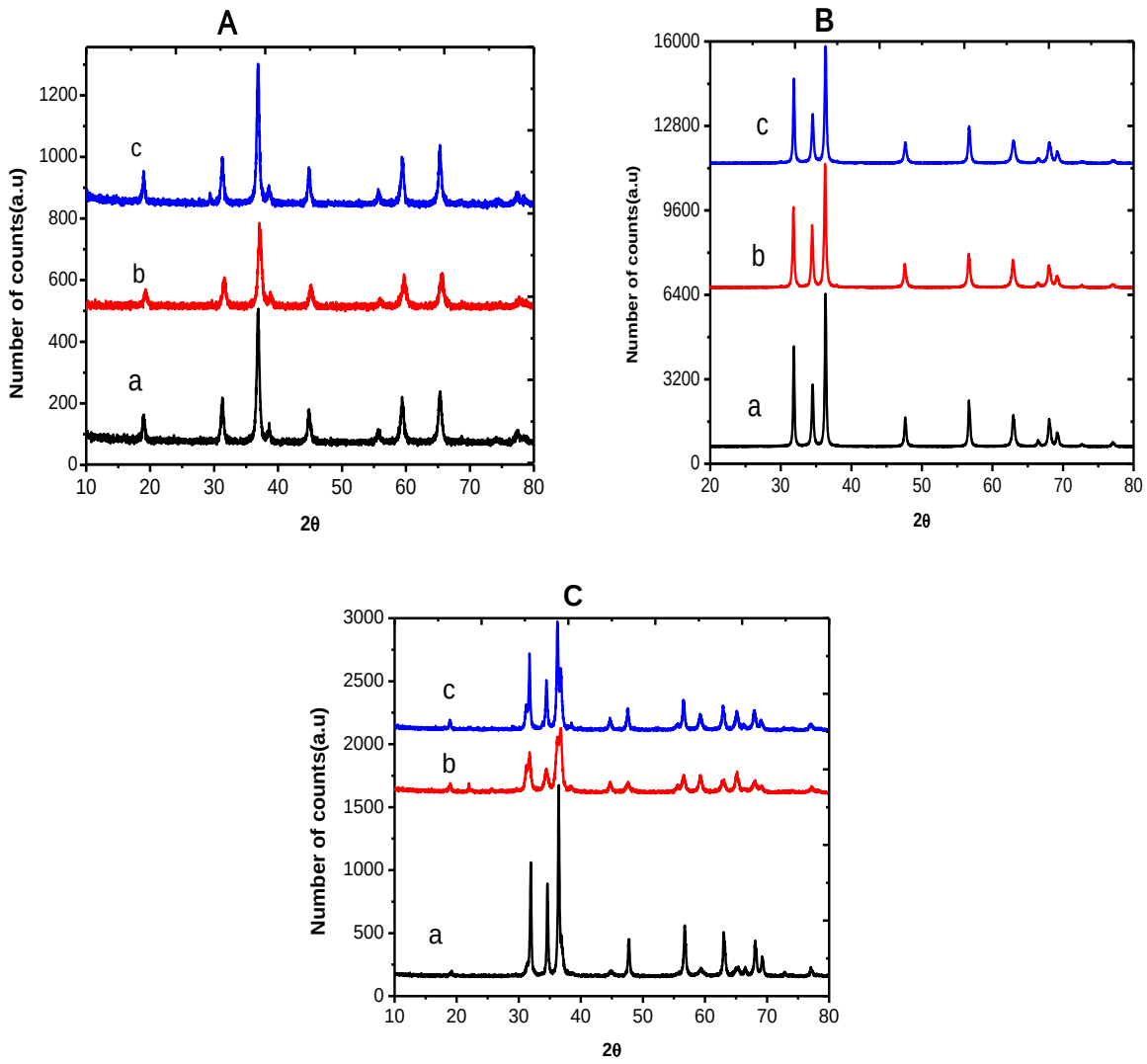

Figure 2. XRD spectra of A) Co_3O_4, B) ZnO NPs and C) Co_3O_4 –ZnO nanocomposite biosynthesized in (a) 1:1, (b) 1:2, and (c) 2:1 ratios of Cobalt nitrate hexahydrate and Zinc acetate dihydrate and their composite, respectively using waste extract of Potato fruit peel.

Figure 3 was also shows XRD pattern of Co_3O_4, ZnO NPs and Co_3O_4-ZnO nanocomposite biosynthesized from cobalt nitrate hexahydrate precursor, zinc acetate dihydrate and their composites and waste extract of banana fruit peel with in three different volume ratios.The formation of biosynthesized Co_3O_4, ZnO NPs and Co_3O_4-ZnO nanocomposite confirmed by X-ray diffraction measurements. The diffraction peaks were observed at 2θ values of (0.4370), (2.2814), (3.0505), (4.1645), (6.2767), (7.1615) for biologically synthesized Co_3O_4, along with miller indices values of (111), (220), (311), (400), (511), (440), respectively and biosynthesized ZnO NPs diffraction peaks were observed at (31.3905), (34.4612), (36.4735), (47.9663), (56.6567), (62.6788) along with miller indices values of ((100), (002), (101), (102), (110), (103), respectively. The formation of biosynthesized Co_3O_4-ZnO nanocomposite was also confirmed by X-ray diffraction measurements and their peaks observed at 2θ values of (31.8057), (34.6678), (36.3926), (47.8407), (56.4395), (63.0834), (68.3603) along with miller indices values of (100), (002), (400), (102), (110), (511), (103).

The average crystalline size for the different kinds of Co_3O_4, ZnO NPs and Co_3O_4-ZnO nanocomposites were estimated as (16.04, 10.70, 12.43), (22.40, 12.79, 20.47), and (21.61, 9.52, 10.09), respectively from the given ratios of 1:1, 1:2 and 2:1 ratios. Thus the broadening of XRD peak of green synthesized nanoparticles observed in our study confirms the size reduction. There is no addition peak in the nanocomposite, indicating no impurity in the synthesis of Co_3O_4-ZnO nanocomposite[100]. Therefore, calcinated nanoparticles Co_3O_4, ZnO and Co_3O_4-ZnO nanocomposite shows sharp peak which confirms good crystallinity of the synthesized nanocomposite

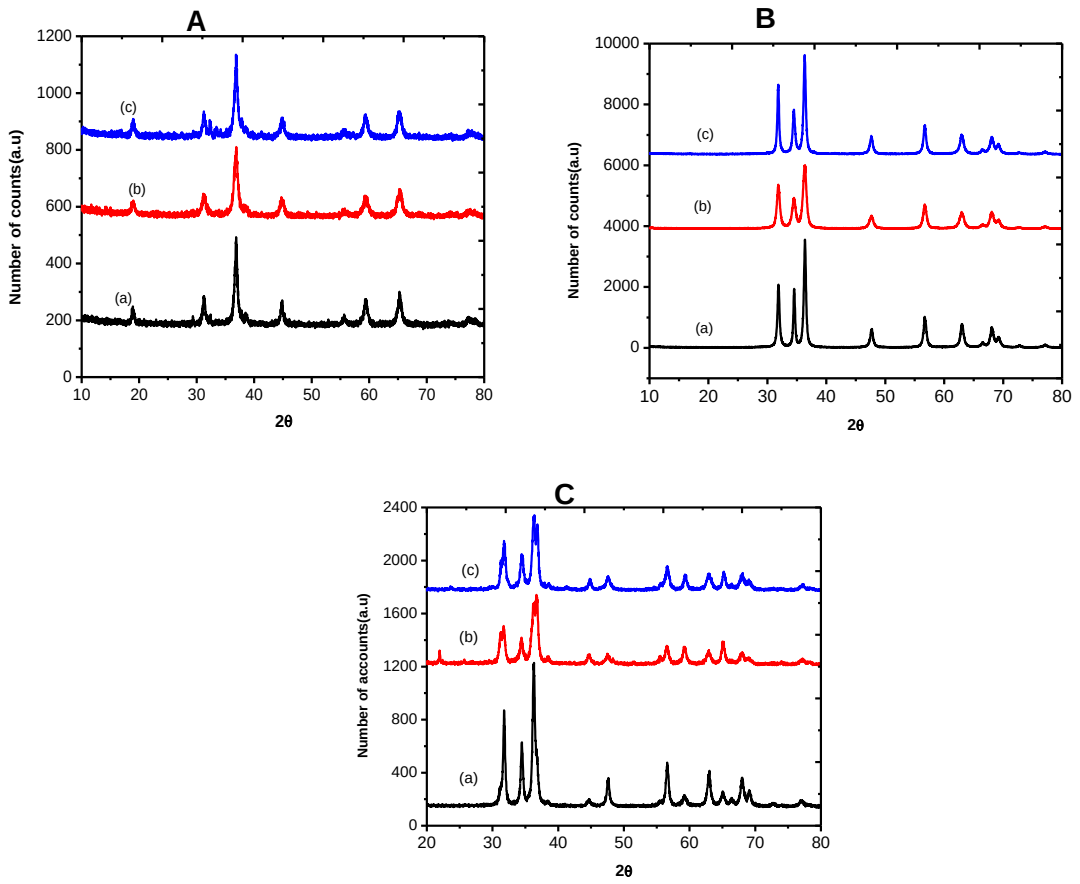

Figure 3: XRD spectra of A) Co_3O_4, B) ZnO NPs and C) Co_3O_4–ZnO nanocomposite biosynthesized in (a) 1:1, (b) 1:2, and (c) 2:1 ratios of Cobalt nitrate hexahydrate and Zinc acetate dihydrate and their composite respectively using waste extract of banana fruit peel.

It is clear indicates that, all the diffraction peaks of ZnO can be indexed to the hexagonal wurtzite structure[101] and peaks corresponds to structured composites consist of different phases. The XRD pattern of structured Co_3O_4 –ZnO composite indicates that it consists of two kinds of phases, hexagonal ZnO and spinel structured cubic Co_3O_4 confirming the coexistence of Zn and Co oxide structure together to form a composite however, the peaks of Co_3O_4 are weak compared with ZnO and it is matched with the data reported[102]. The Figure 4 (A and B) shows the optimized ratios of waste extract fruits peel average crystallite size of Co_3O_4 , ZnO nanoparticles and Co_3O_4 -ZnO nanocomposites synthesized within a 1:2 ratios which has a relatively smaller particle size compared to the remaing ratios of average crystalline size .This is due to the fact that the greater amount of the extract used during the synthesis process results in

more stabilizing agents that in turn effectively stabilize the biosynthesized Co_3O_4 , ZnO and Co_3O_4 -ZnO nanocomposites during the synthesis process. The peaks of three of the XRD spectra are in good agreement with the literature reported before [103, 104].

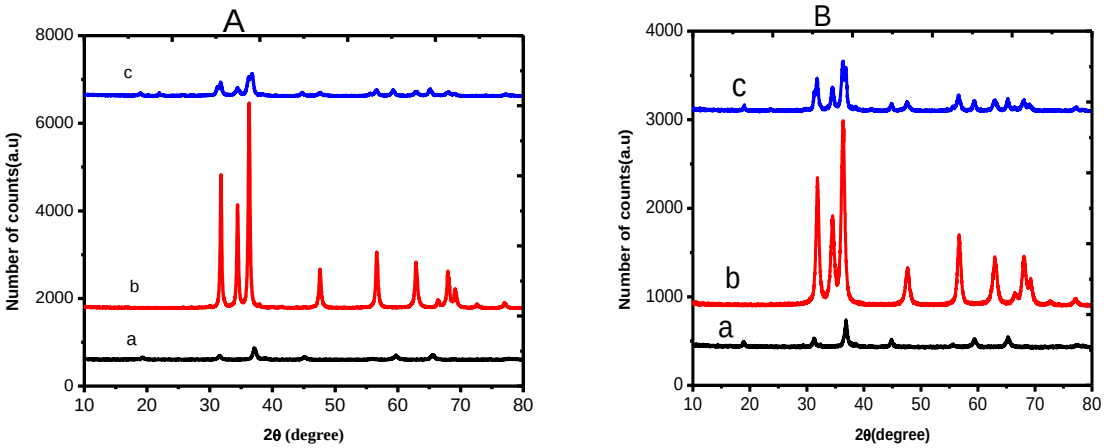

Figure 4: XRD spectra of (A) optimization from potato fruit peel and (B) Optimization from banana fruit peel (a) biosynthesized Co_3O_4, (b) biosynthesized ZnO and (c) biosynthesized Co_3O_4 - ZnO within 1:2 ratio.

The Co_3O_4-ZnO sample that the product was well crystalline having no impurity as there was no unmatched peak. All the peaks of the final product are matched either with Co_3O_4 or ZnO. Interestingly compare to the peak intensity of pure Co_3O_4, the peak intensity of Co_3O_4-ZnO for Co_3O_4 phase was noticeably strong. The peak intensity of the ZnO phase is much stronger than the Co_3O_4 phase in the final product for the two materials using waste extract of potato and banana fruits peel. As it can be observed above for the XRD spectrum (B), Co_3O_4, (1:2) NPs their crystalline nature sharp peak intensity was less than XRD spectrum (A) due to the addition of an excessive amount of the waste extract of banana fruit peel.

Figure 5 shows XRD pattern of Uncalinated (A) Co_3O_4 NPs, (B) ZnO NPs and (C) Co_3O_4-ZnO nanocomposite biosynthesized from cobalt nitrate hexahydrate precursor, zinc acetate dihydrate and their composites and waste extract of potato (a) and banana (b) fruits peel with in different volume ratios. Both Uncalcinated biologically synthesized cobalt oxide and zinc oxide nanoparticles using waste extract of potato and banana not show sharp peak and also

uncalcinated Co_3O_4-ZnO nanocomposite the biologically synthesized specially not show sharp peak one the crystallinity was absent due to excess plant extract used.

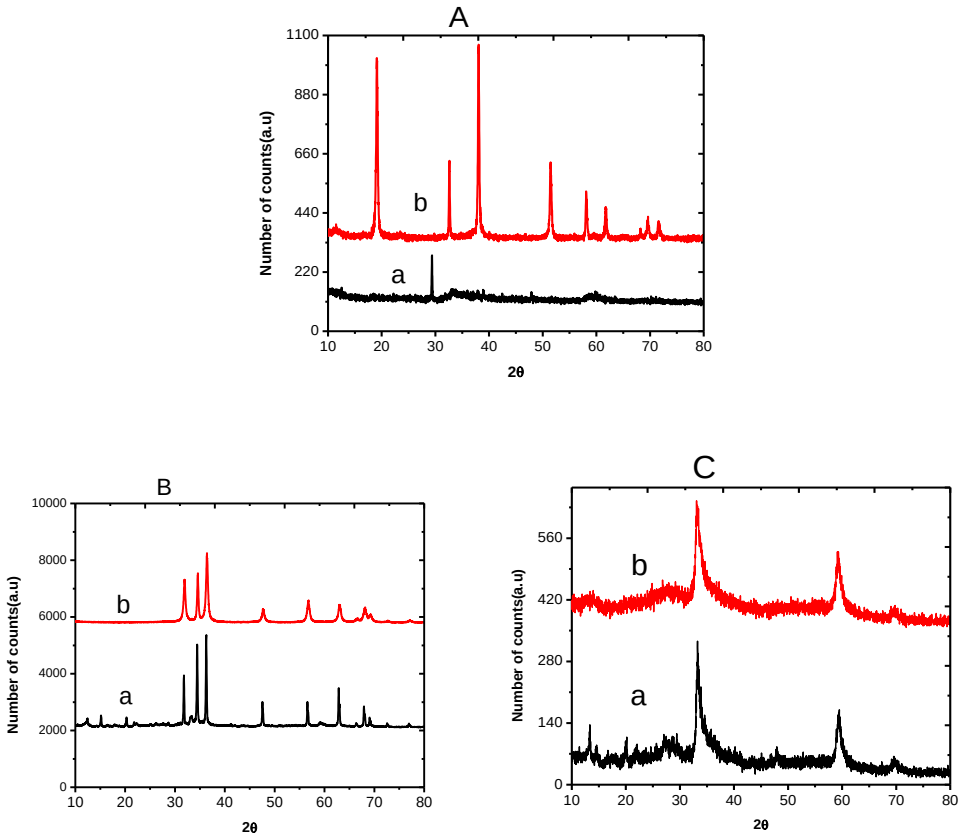

Figure 5: XRD pattern of Uncalcinated(A) biosynthesized Co_3O_4 NPs, (B) ZnO NPs and (C) biosynthesized Co_3O_4 -ZnO nanocomposites in the presence of extract of peels of potato(a) and banana(b).

4.3. SEM Analysis

SEM analysis was carried out to find the surface morphology of cobalt oxide, zinc oxide, and Co_3O_4 -ZnO nanocomposite using JCM-6000 scanning electron microscope at different magnification levels and results were shown in Figures 6 and 7. The micrographs Figures 6 (A, B and and C) showed that the particles were found to be spherical shape.

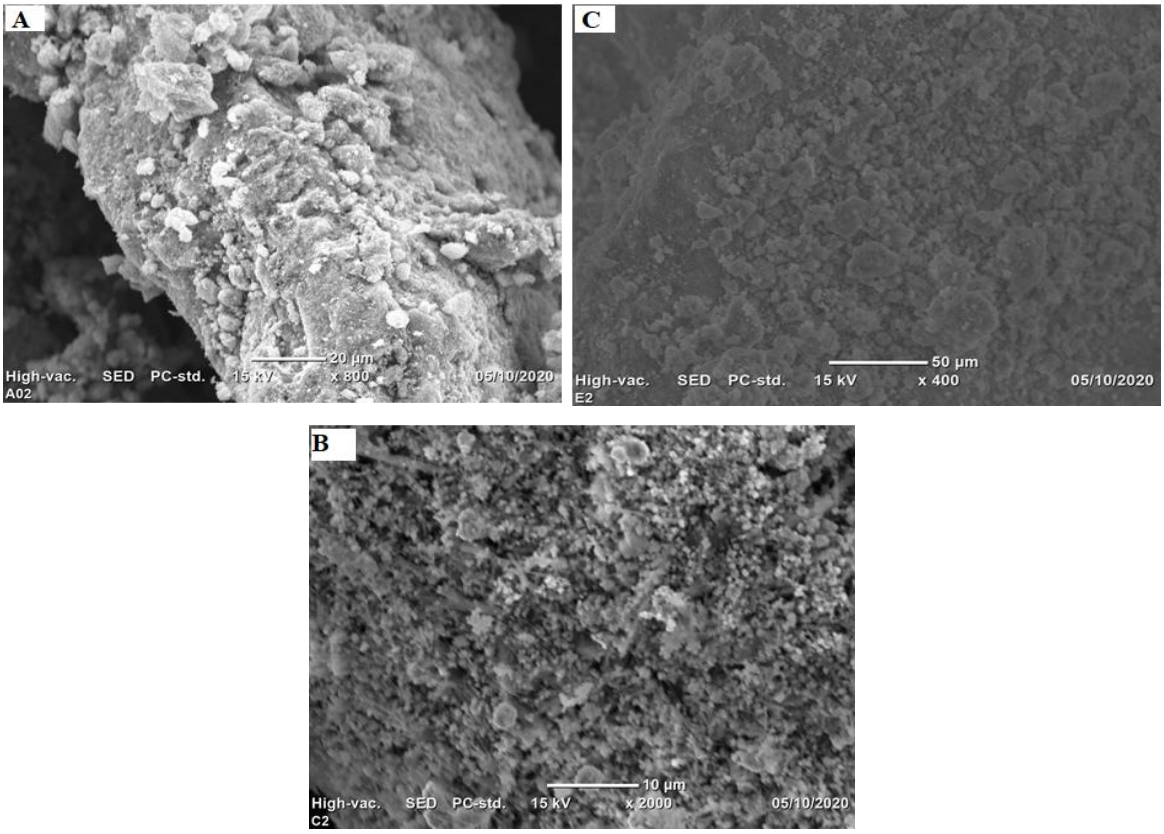

Figure 6: Scanning electron micrograph (SEM) image of (A) Co_3O_4, (B) ZnO and (C) Co_3O_4-ZnO composite in the presence of extract of potato peel.

Figure 7 also elucidates the decrease of particles size with the biologically synthesized using extract of banana peel implies the well association of biomolecules obtained from the fruit extracts with that of Co_3O_4 and ZnO precursor salt and their composites during the biosynthesis process.

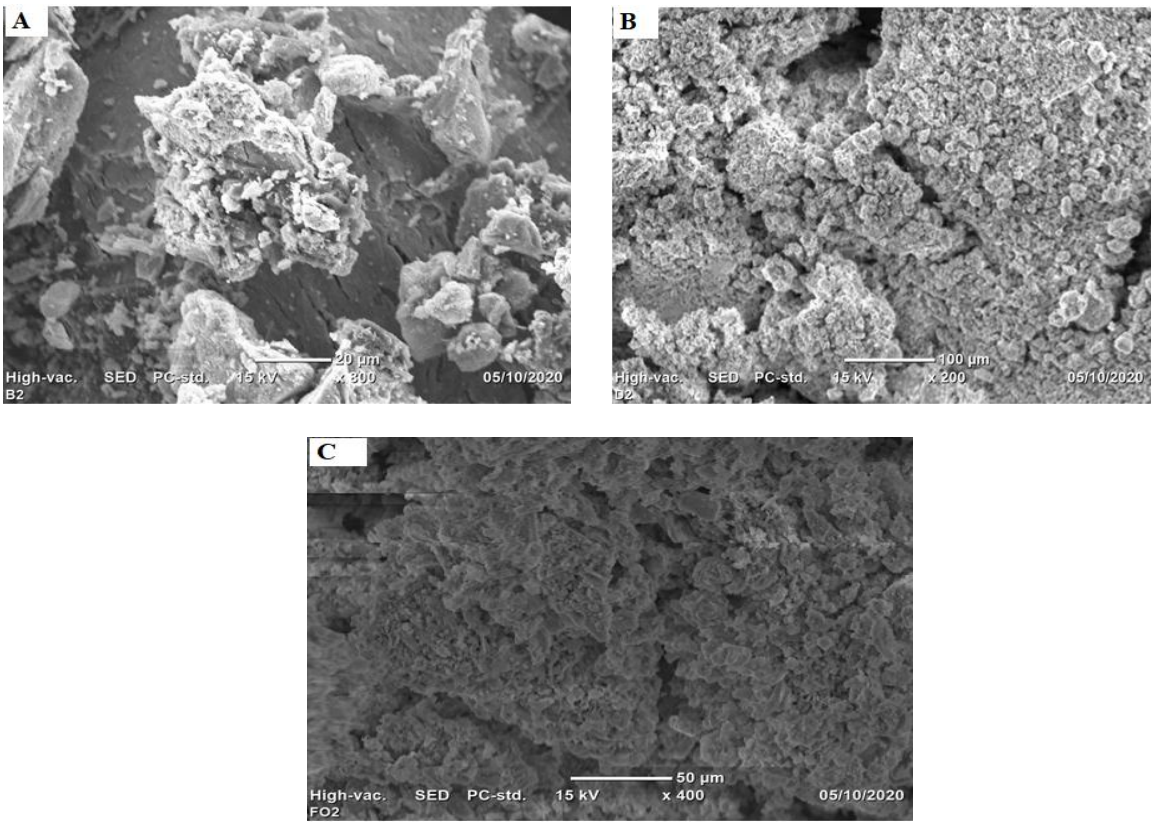

Figure 7: Scanning electron micrograph (SEM) image of (A) Co_3O_4, (B) ZnO and (C) Co_3O_4-ZnO composite in the presence of extract of banana peel.

4.4. Ultraviolet-Visible Spectroscopy (UV-Vis DRS) Analysis

The band gap energy of synthesized nanoparticles was estimated by using ultra violet visible diffuse reflectance spectroscopy (UV –Vis DRS). The band gap is the minimum energy needed for an electron to be excited from the top of the valence band to the bottom the conduction band. Once that minimum energy is reached then the sample can start absorbing light and electrons are excited from the valence band to the conduction band. The bandgap energy was determined based on the numerical derivative of the optical absorption coefficient using Tauc's plot method equation by plotting $(\alpha h\nu)^2$ against $h\nu$ as shown in Figure 8. The bandgap energy of Co_3O_4 NPs was found to be 3.25 , 3.33, and 3.37 eV for the 1:1, 1:2, and 2:1 volume ratios of Co precursor salt and potato peel extract, respectively and 3.60, 3.74, and 3.81 eV for the 1:1, 1:2, and 2:1 volume ratios of Co precursor salt and banana peel extract, respectively. The variation in the E_g

for the different kinds of biosynthesized Co_3O_4 NPs is due to the variation in volume ratio between Co precursor salt and the peel extract that leads the biosynthesized Co_3O_4 NPs to absorb at different regions of UV-Vis light. Broadening of the spectrum indicates the polydispersed nature of the biosynthesized nanoparticles and the black shift of the absorption curve results in the reduction of the bandgap energy. If the size of the particle is very small light interacts with the samples instead of absorption with parts of the light scattered and reflected.

UV-Vis spectroscopy result showed that the typical peaks of Co_3O_4 NPs were detected in the range of maximum wavelength between 427-741 nm Co precursor salt and potato peel extract and 436-728 nm Co precursor salt and banana peel extract as shown in Figure 8.These peaks indicated the transfer processes of Co (II) and Co (III) with oxygen, respectively[105]. Among them the incorporation of Co_3O_4 NPs with bandgap of 3.25eVand 3.60eV using extract of potato and banana fruits peel, respectively leads to a narrow band gap of the material.

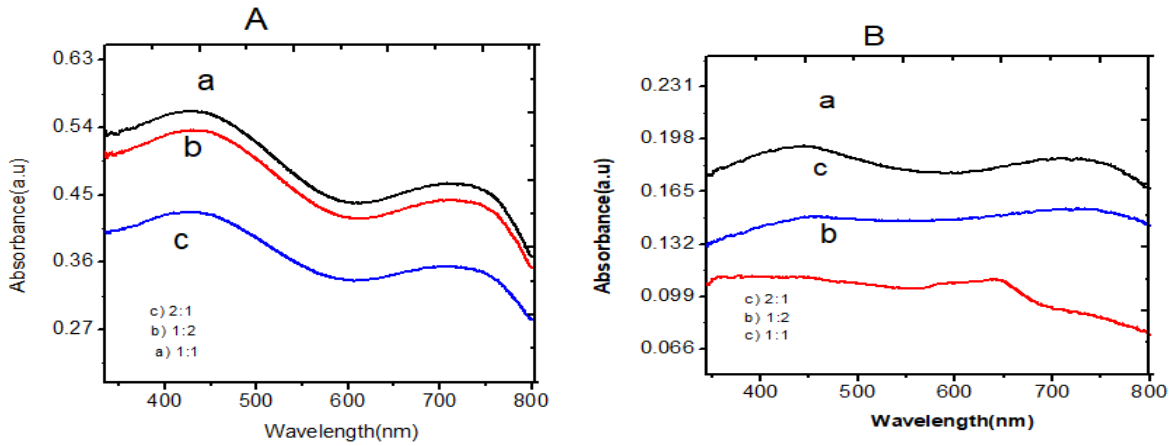

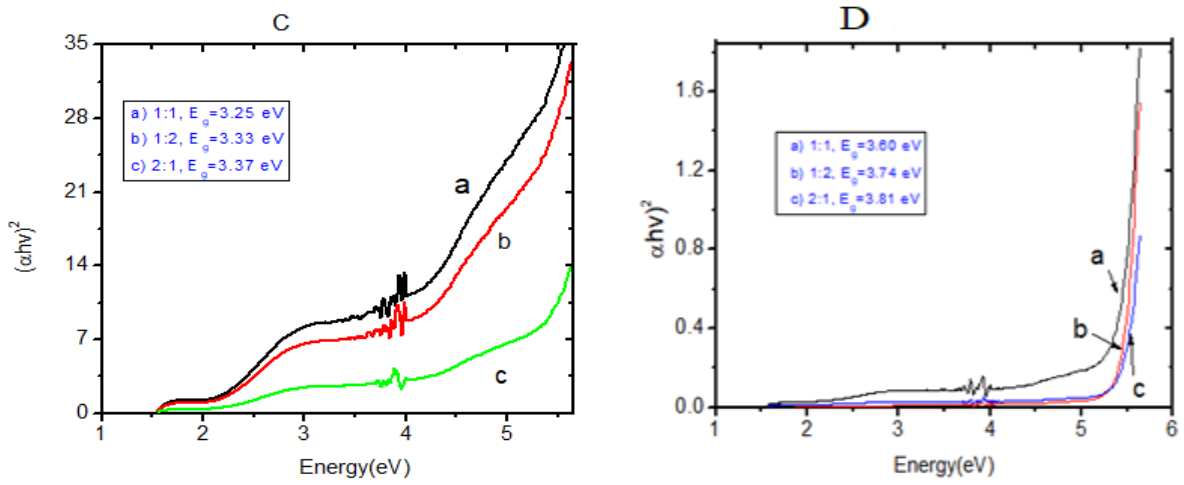

Figure 8. (A and B) UV-Vis absorption spectra and (C and D) Tauc plot of Co_3O_4 NPs synthesized from cobalt nitrate hexahydrate and waste extract of (potato and banana) fruits peels, respectively.

Figure 9 shows the UV–visible absorption spectrum of ZnO NPs is revealed that the dispersing ZnO nanoparticles. UV-Visible spectroscopy is most widely used technique to investigate the optical properties of the particles. UV-Visible spectroscopy analysis was done in the range of 200-800 nm. Zinc oxide nanoparticles typically exhibit optical absorption around 370 nm [106, 107]. The optical absorbance spectra of zinc oxide nano powder showed in figure 9 (A and B). The band was observed at 362 and 362 nm assigned to the absorption of zinc oxide nanoparticles with extract of potato and banana fruits peel, respectively.

The calculated band gap of ZnO NPs was once to be 3.32 eV, which was contract with the previously mentioned work [108, 109]. As shown in Fig. 10, the band gap energies estimated from the intercept of the tangents to the plots are 3.08eV, 3.12eV and 3.16eV for pure ZnO using extract of potato fruit peel whereas 3.17eV, 3.28eVand 3.24eV for ZnO using extract of banana fruit peel . It indicates that the incorporation of ZnO with band gap of 3.08eVand 3.17eV using extract of potato and banana fruits peel, respectively leads to a narrow band gap of the material.

In addition, reducing the width of the band gap can increase the utilization of visible light. The variation in the E_g for the different kinds of biosynthesized ZnO NPs is due to the variation in volume ratio between Zn precursor salt and the waste extract of potato and banana fruits peel that leads the biosynthesized ZnO NPs to absorb at different regions of UV-Vis light.

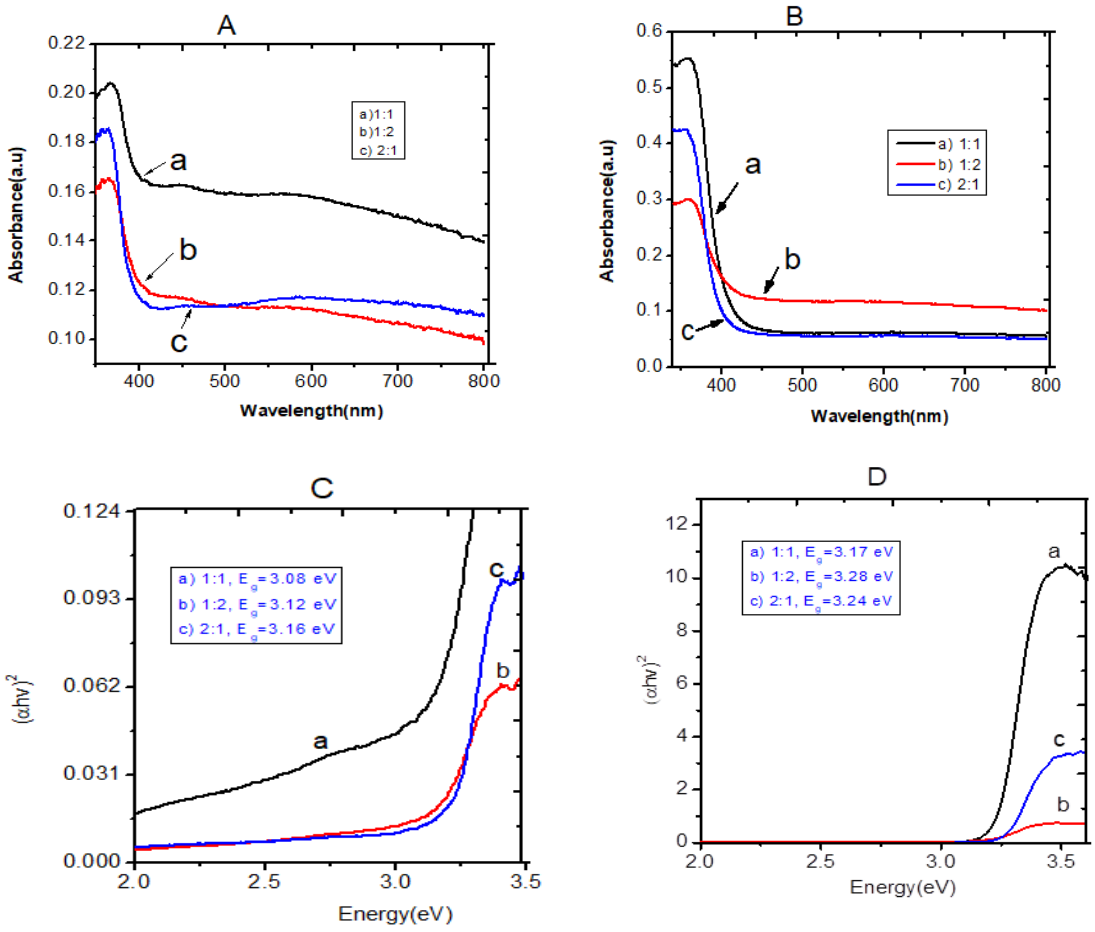

Figure 9. (A and B) UV-Vis absorption spectra and (C and D) Tauc plot of ZnO NPs synthesized from zinc acetate dihydrate and waste extract of (potato and banana) fruits peels, respectively.

The DRS UV-Vis spectra of as-synthesized Co_3O_4-ZnO nanocomposites were recorded to determine their light absorption characteristics and Figure 10 shows the DRS UV-Vis spectra of structured nanocomposites. Figure 10(D) Co_3O_4-ZnO shows the highest visible light absorption while Figure 10(C) shows the lowest visible light absorption. Obviously, the band gap of the three ratios of composite structures followed by the trend of Co_3O_4-ZnO (b) (3.48 eV) > Co_3O_4-ZnO(c) (3.37eV) > Co_3O_4-ZnO (a) (3.33eV). Spectra of light absorption (D) also followed by the

trend of Co_3O_4-ZnO (c) (3.81eV) > Co_3O_4-ZnO (a) (3.72eV) > Co_3O_4-ZnO (b) (3.56eV) with the ratios of composites.

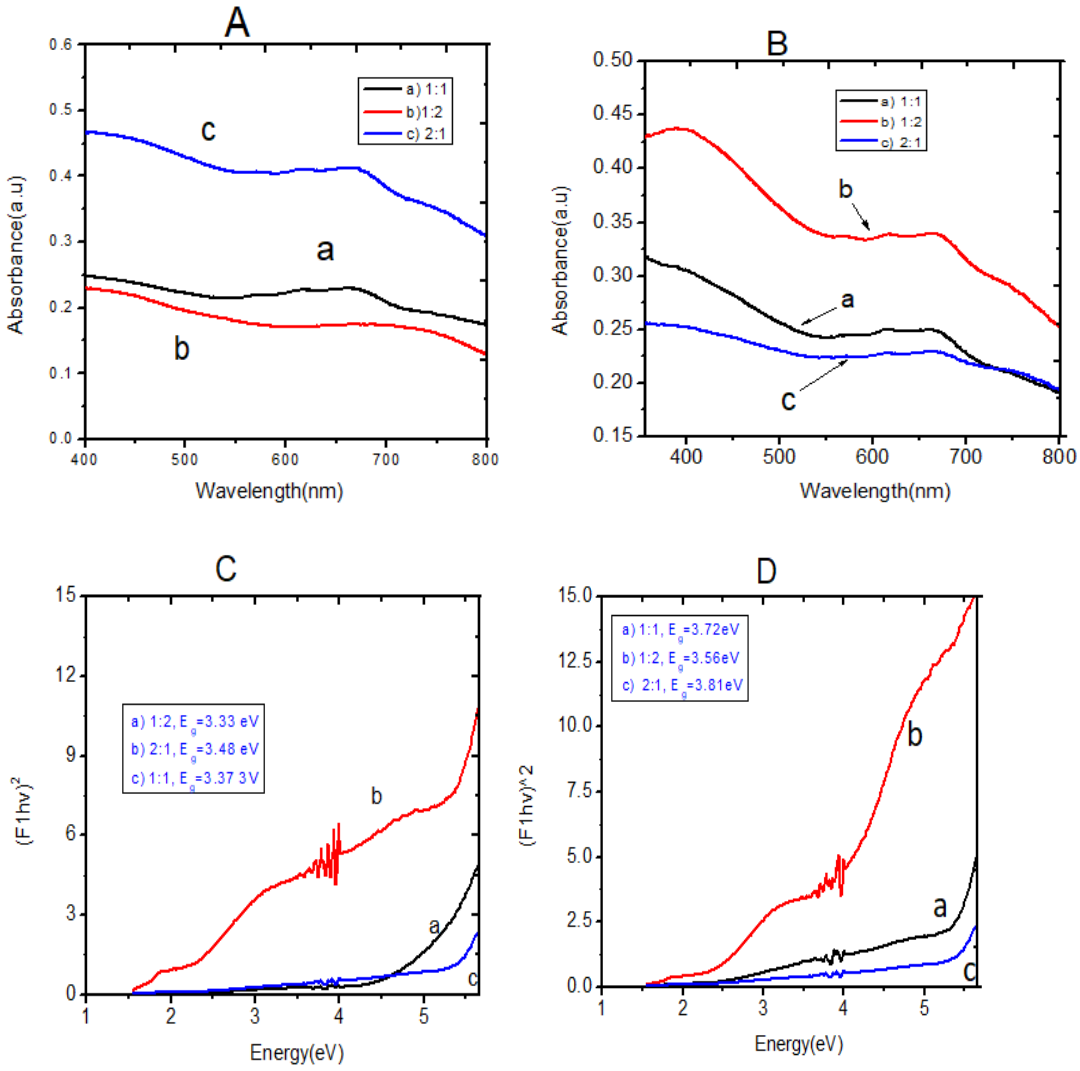

Figure 10. Graph (A and B) UV-Vis absorption spectra and (C and D) Tauc plot of ZnO as a result of the addition of Co_3O_4.

Figure 11 shows the UV-Vis absorption characteristics of the pure Co_3O_4, ZnO and Co_3O_4-ZnO nanocomposite. Co_3O_4 nanoparticles present two broad peaks, originated at around 427 nm and 741 nm. These two band gap absorption peaks are quite close to the recorded band energies of the other reported Co_3O_4 systems[110, 111]. The multiple band gaps for the Co_3O_4 nanoparticles is attributed to the possibilities of O^{2-} to Co^{2+} and O^{2-} to Co^{3+} charge-transfer processes in Co_3O_4

nanoparticles as observed in Co_3O_4 quantum dot in cubic morphology [112]. ZnO shows near band edge absorption peak at around 368 nm. Middle panel of Figure 11 shows the absorbance characteristics of Co_3O_4-ZnO nanocomposites sample. After formation of the nanocomposite the intense peaks of Co_3O_4 has been lost and weak peaks, originated from Co_3O_4, are observed at around 765 nm and around 485 nm. The sharp peak in the UV region at around 365 nm is originated from the band edge transition of ZnO. The wavelength shifting of the Co_3O_4 peak positions in the Co_3O_4-ZnO nanocomposite is attributed to the surface defect states caused by the local lattice mismatch after shell formation.

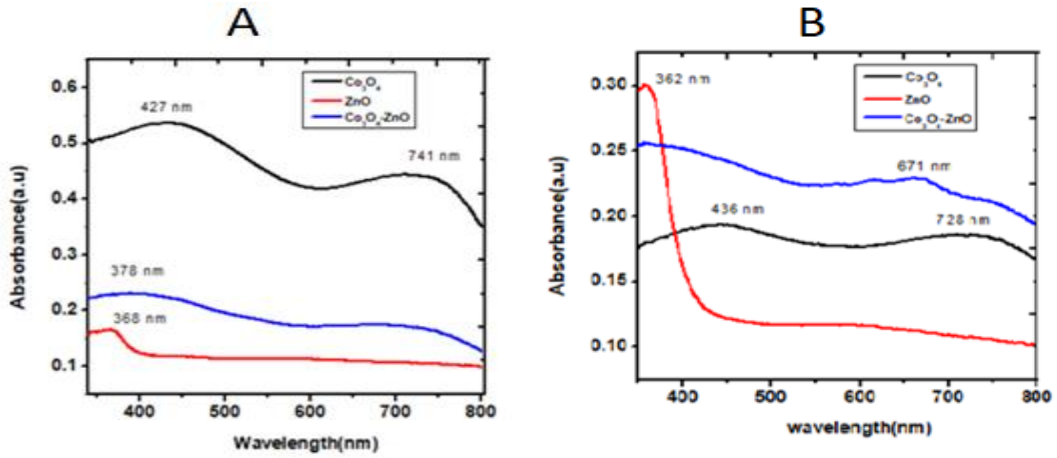

Figure 11.Optical absorbance spectrum for Co_3O_4-ZnO nanocomposite (middle panel) and same for (lower panel) ZnO and Co_3O_4 samples (upper panel).

4.5. Fourier Transform Infrared (FTIR) Analysis

FTIR spectrophotometer was used to analyze the functional group of Co_3O_4, ZnO, and Co_3O_4-ZnO nanocomposite. The wavelength of 4000-400 cm^{-1} was used for the analysis of functional groups of samples, and the results can be seen in figure 12 and 13. Functional groups of Co_3O_4, ZnO, Co_3O_4-ZnO nanocomposite, extract of potato and banana fruits peel powder with FTIR spectrophotometer can be seen in figure 12. The -OH functional groups could be observed at the frequency of 3500-3000 cm^{-1}, the peak at 3438cm^{-1} could be observed at the sample of Co_3O_4, ZnO, and Co_3O_4-ZnO nanocomposite. The C=O functional group could be observed at the wavenumber of 1840.11$cm^{-1}$for extract of potato fruit peel powder,1633.62 for extract of banana

fruit peel powder, 1780.45 cm^{-1} for Co_3O_4 and 1793.86 for ZnO. The wavenumber of 2854.65 cm^{-1}, 2862.36 cm^{-1}, 2924.09 cm^{-1} and 2931.80 cm^{-1} are the C-H functional group according to the reference[113] that reported the C-H group appeared at wavenumber of 2923.76 cm^{-1} and 2933.18 cm^{-1}. The C=O and C-H groups appeared because the synthesis used the precursor of Zn $(CH_3COO)_2.2H_2O$ that was not perfectly decomposed to ZnO and precursor of $Co(No_3)_2.6H_2O$ was not perfectly decomposed to Co_3O_4.

The wavenumber of 524.59 cm^{-1} is assigned to Zn-O bond similar to another report [113] that the vibration Zn-O appeared at wavenumber of 424.26 cm^{-1}, 471.36 cm^{-1} and 542.86 cm^{-1}. FT-IR measurements were carried out to identify the major functional groups on the BPE and PPE surface and their possible involvement in the synthesis and stabilization of Co_3O_4, ZnO nanoparticles. Control spectrum (BPE and PPE treated with Co_3O_4, ZnO) showed several peaks indicating the nature of the biological material. Banana peels are mainly composed of pectin, cellulose and hemicelluloses [114] and associated with the functional groups. The aqueous extract of potato peel is rich in various phenolic acids, including hydroxycinnamic acids and flavonoids, which have strong antioxidant capacity[115].

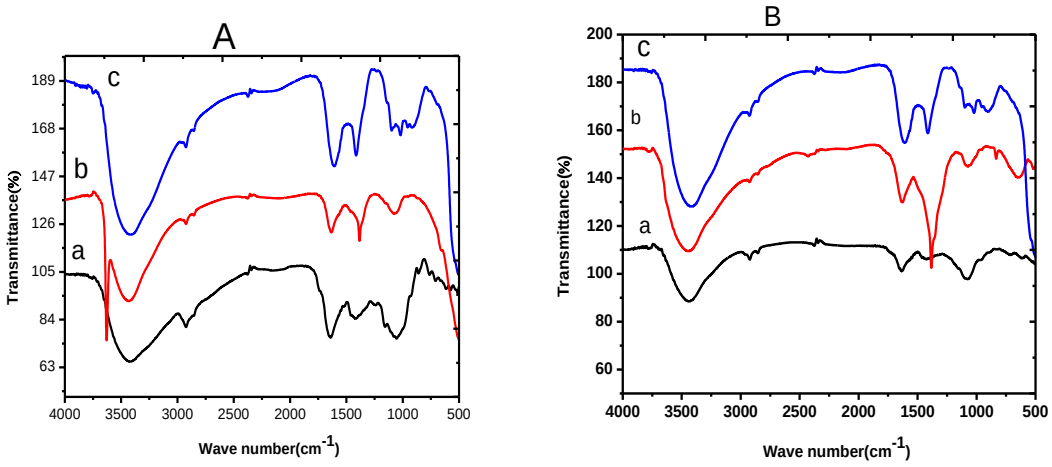

Figure12**.** FTIR spectra of (A) Uncalcinated synthesised (a) dried waste extract of potato fruit peel powder,(b) Co_3O_4 and (c) ZnO NPs and (B) Uncalcinated synthesised (a) dried waste extract of banana fruit peel powder ,(b) Co_3O_4 and (c) ZnO NPs.

Figure 13 shows Calcinated synthesized Co_3O_4 and ZnO NPs (A) extract of potato peel and (B) extract of banana peel. The strong bands at 564 cm^{-1} and 851cm^{-1} for extract of potato fruit peel and 557 cm^{-1} and 837cm^{-1} for extract of banana fruit peel belonging to the spinel structure of the Co_3O_4 NPs. The broad peaks located in between 851-664 cm^{-1} and 838-658 cm^{-1} are attributed to the stretching vibration mode of Co-O in which Co is Co^{2+} and are tetrahedral coordinated. The later one at 564 and 557 cm^{-1} can be assigned to Co-O of octahedral coordinated Co^{3+}. In Co spectrum, the two absorption peaks at 652 and 549 cm^{-1} originate from the stretching vibration of the Co−O bond where Co^{2+} ($3d^7$) is tetrahedrally coordinated at 653 cm^{-1} and Co^{3+} ($3d^6$) is octahedrally coordinated at 550 cm^{-1} confirming the presence of spinel Co_3O_4 [116, 117].

The vibration in the range of 400−700 cm^{-1} generally corresponds to metal−oxygen bonding. The two bands appeared at 3631 and 1406 cm^{-1} have been assigned to the stretching and binding vibrations of absorbed water molecule with Co_3O_4 NPs [118]. The wavenumber of 524.59 cm^{-1} is assigned for both calcinated synthesized ZnO NPs using waste extract of potato and banana fruits peel to Zn-O bond similar to another report [113] that the vibration Zn-O appeared at wavenumber of 424.26 cm^{-1}, 471.36 cm^{-1} and 542.86 cm^{-1}. Figure 13 (C) shows calcinated biosynthesized Co_3O_4-ZnO nanocomposites. The wavenumber of functional groups shifted Co_3O_4-ZnO formation as shown in Figure 13 (C). By adding the Co_3O_4 to ZnO, the shift wavenumber at the frequency of 750-400 cm^{-1} could be observed. The wavenumber of 517 cm^{-1} and 537$cm^{-1}$was found in the biosynthesized Co_3O_4-ZnO using waste extract of potato fruit peel and biosynthesized Co_3O_4- ZnO using waste extract of banana fruit peel, respectively. The shift of wavenumber indicated that the addition of Co_3O_4 may change the structure of ZnO. Three types of spectra have almost similar peaks except that in case of plant extract containing NPS, there was slight shifting and broadening of peaks.

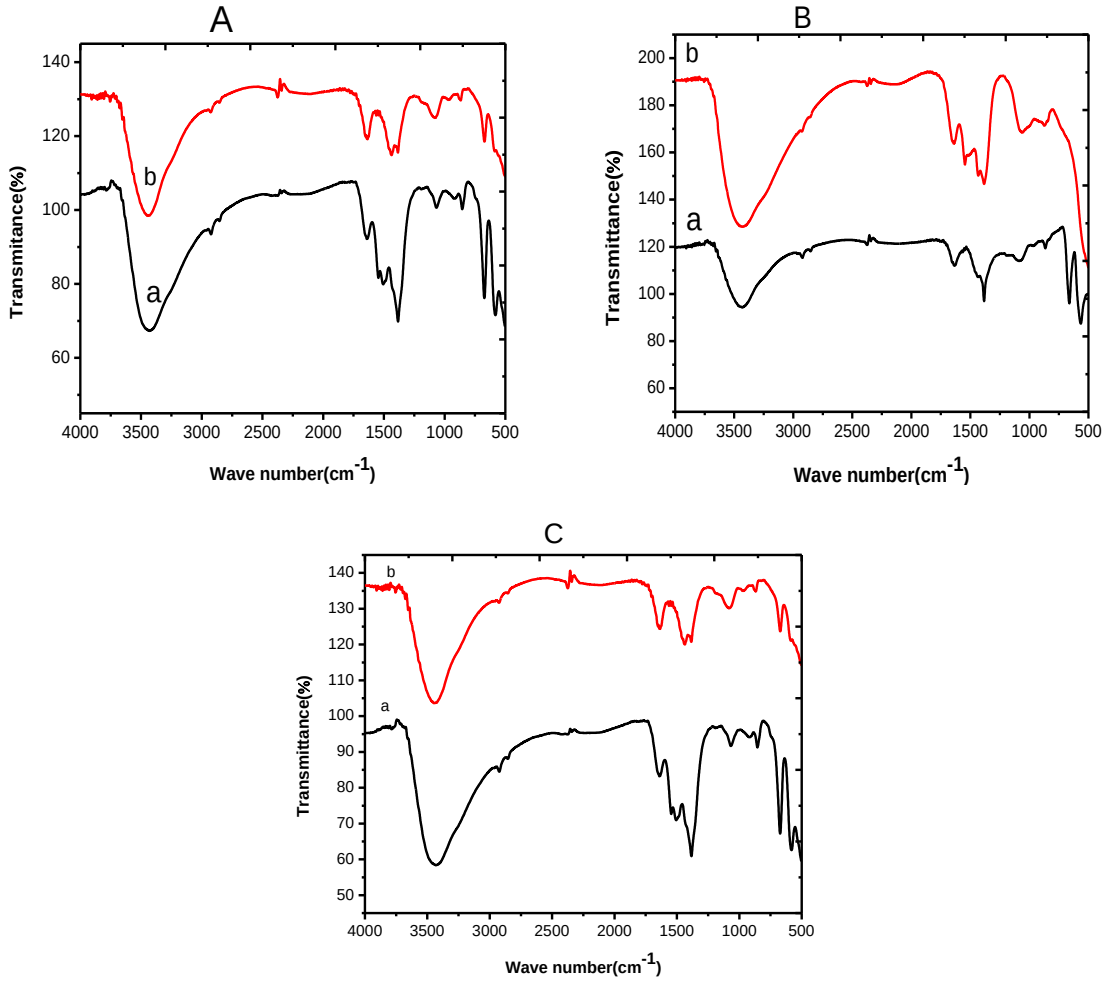

Figure 13**.** FTIR spectra of Calcinated synthesized Co_3O_4 and ZnO NPs (A) using waste extract of potato fruit peel and (B) material using waste extract of banana fruit peel), and (C) biosynthesized Co_3O_4- ZnO from a) From Potato and Banana fruits peels (after calcination).

4.6. Antibacterial studies

Table 1 and 2 Co_3O_4, ZnO nanoparticles and Co_3O_4- ZnO nanocomposite at concentrations of 50mg/ml, 75mg/ml and 100mg/ml were tested for antibacterial activity using gram-negative and gram-positive bacteria strains of (*Escherichia coli* and *Klebsiella pneumonia*) and (*Staphylococcus aureus* and *B.subtilis*), respectively for biologically synthesized Co_3O_4- ZnO nanocomposite using disc diffusion method. Among the different ratios of the biosynthesized Co_3O_4, ZnO and Co_3O_4- ZnO nanocomposite, Co_3O_4, ZnO and Co_3O_4- ZnO (1:2) synthesized

using both waste extract of potato and banana fruits peel shows better performing antibacterial activity as compared to the remaining two ratios. Green synthesized ZnO NPs and Co_3O_4-ZnO nanocomposite show antibacterial activity because biomolecules obtained from the waste extract of potato and banana fruits peel are giving excess electron to ZnO and Co_3O_4- ZnO and result in the formation of superoxide radicals O^{2-}, and the superoxide radicals produce reactive oxygen species (ROS) in bacterial cell [119]. These are all of the reasons for electron production from ZnO NPs and Co_3O_4- ZnO nanocomposite, and as a result, ZnO NPs and Co_3O_4- ZnO nanocomposite show antibacterial activity against both Gram-negative and Gram positive bacteria strains [120] .

Figure 14 showed below the inhibitory of Co_3O_4 was different between the bacteria *Escherichia coli ,Staphylococcus aureus ,Klebsiella pneumonia* and *B.subtilis* using extract of potato fruit peel. Among the different given bacterias, *B.subtilis* better than the remaing three bacterias. Figure 14 also showed that the ZnO was resistant as antibacterial against *K. pneumonia,S. aureus* , and *B.subtilis* and better at inhibiting the growth of bacteria against *Escherichia coli*. Therefore, the Co_3O_4- ZnO nanocomposite can be used as inhibitors of the bacterial growth of *Escherichia coli*. Figure 15 showed that the inhibition zone of ZnO was better antibacterial properties against *B.subtilis* whereas Co_3O_4 was better antibacterial properties against *Escherichia coli*[121]. The antibacterial activity increased by the increase of Co_3O_4 on the composites, indicating that the Co_3O_4 increases the photocatalytic properties of composite. The surface area of Co_3O_4-ZnO nanocomposite may influence the antibacterial activity. Other researchers[122] reported that the larger surface area of Co_3O_4- ZnO was easily enter to the cell and kill the bacteria due to increase of Zn^{2+} ions and reactive oxygen species (ROS).

The antibacterial activity of Co_3O_4, ZnO nanoparticles and Co_3O_4- ZnO nanocomposite were compared with the positive control Erythromycin; the results of antibacterial studies clearly suggest that Co_3O_4, ZnO nanoparticles and Co_3O_4-ZnO nanocomposite synthesized using extracts of potato fruit peel shows even at 100mg/ml has better antibacterial activity than Co_3O_4, ZnO nanoparticles and Co_3O_4-ZnO nanocomposite synthesized using extracts of banana fruit peel. According to several studies, it is believed that metal oxides carry positive charge while bacteria carry negative charges; this causes electrostatic attraction between bacterial cells and metal oxide NPs, which leads to oxidization and finally death of microorganisms [120].

Figure14. Antibacterial activity of biologically (A2) ,(C2)and (E2)synthesized Co_3O_4 , ZnO NPs and Co_3O_4-ZnO nanocomposite, respectively using extract of potato fruit peel 50mg/ml, 75mg/ml and 100mg/ml.

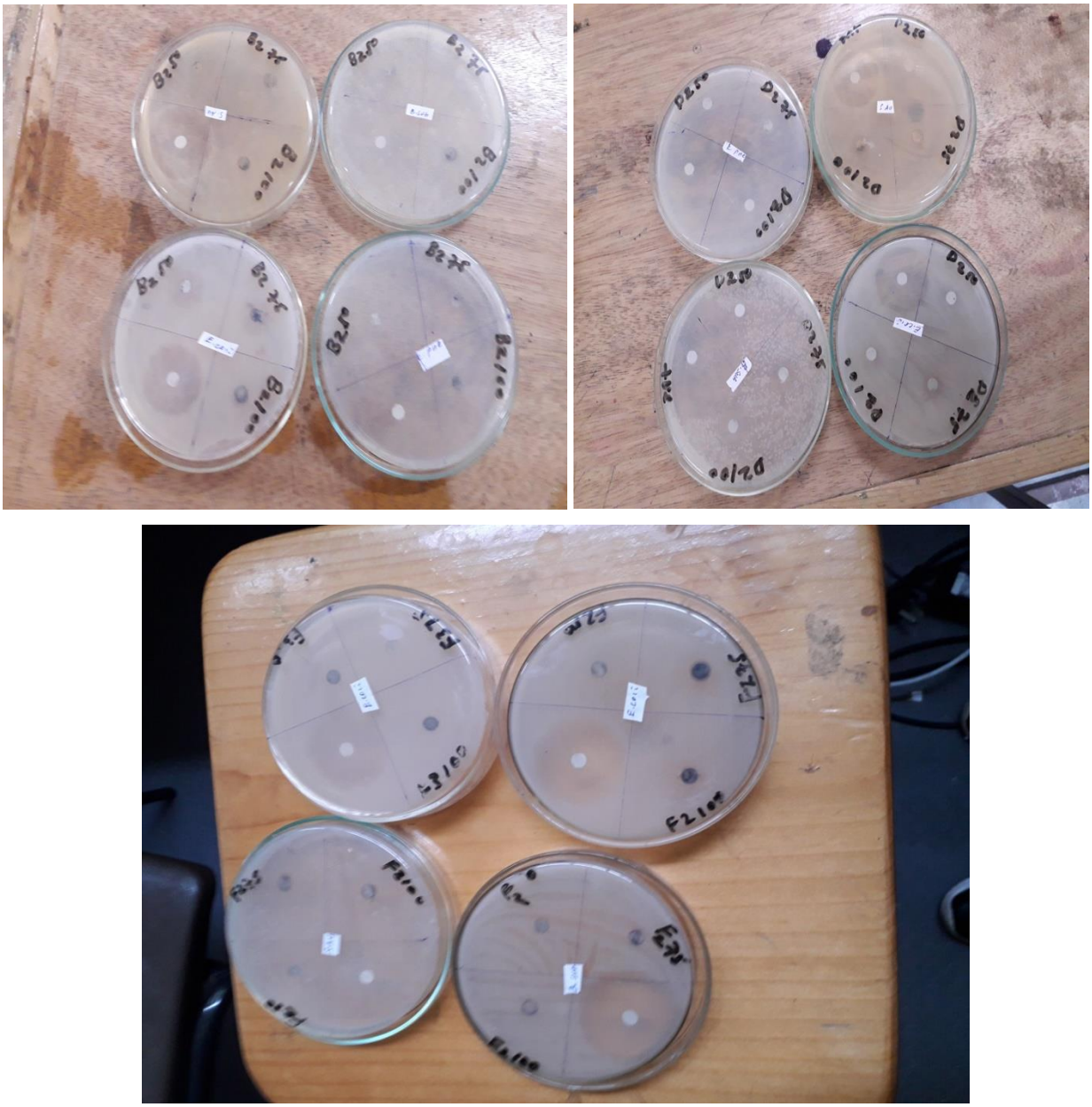

Figure15. Antibacterial activity of biologically (B2) ,(D2)and (F2) synthesized Co_3O_4,ZnO NPs and Co_3O_4-ZnO nanocomposite, respectively using extract of banana fruit peel 50mg/ml, 75mg/ml and 100mg/ml.

Table1. Antibacterial activity of Co_3O_4, ZnO and Co_3O_4 -ZnO nanocomposite biosynthesized within 1:1, 1:2, and 2:1 ratios of cobalt nitrate hexahydrate, zinc acetate dihydrate and their composite, respectively with waste extract of potato fruit peel against Staphylococcus aureus, Escherichia coli, Klebsiella pneumonia, and B.subtilis bacteria strains (at the concentration of 50, 75 and 100 mg/mL of Co_3O_4, ZnO and Co_3O_4 -ZnO nanocomposite).

Precursor salt : fruits peel extract	Zone of inhibition (mm)				
	Conc.(mg/ml)	*E.coli*	*K.pneumoniae*	*B.subtilis*	*S.aureus*
Co_3O_4(1:1)	50, 75, and 100	6,6,6	6,25,20	0.9,6,6	6,6,6
Co_3O_4(1:2)	50, 75, and 100	6,6,6	27,22,6	0.8,6,6,	6,6,6
Co_3O_4(2:1)	50, 75, and 100	0.6,6,6	24,16,6	6,6,6	6,6,6
ZnO(1:1)	50, 75, and 100	10 ,14, 18	6,6,6	12,19,25	6,6, 10
ZnO(1:2)	50, 75, and 100	6,6,31	6,6,6	6,6,6	6,6,6
ZnO(2:1)	50, 75, and 100	8,10,18	25,19,6	6,6,25	6,6,16
Co_3O_4-ZnO(1:1)	50, 75, and 100	6,6,6	10,12,6	6,6,6	6,6,6
Co_3O_4-ZnO(1:2)	50, 75, and 100	6,6,12	6,6,6	6,6,18	6,6,30
Co_3O_4-ZnO(2:1)	50, 75, and 100	6,6,6	6,6,6	6,6,6	6,6,6
Erythromycin(+ve) control		28	28	24	24

Table2. Antibacterial activity of Co_3O_4, ZnO and Co_3O_4-ZnO nanocomposite biosynthesized within 1:1, 1:2, and 2:1 ratios of cobalt nitrate hexahydrate , zinc acetate dihydrate and their composite, respectively with waste extract of banana fruits peel against Staphylococcus aureus, Escherichia coli, Klebsiella pneumonia, and B.subtilis bacteria strains (at the concentration of 50, 75 and 100 mg/mL of Co_3O_4, ZnO and Co_3O_4 -ZnO nanocomposite).

Precursor salt : fruits peel extract	Zone of inhibition (mm)				
	Conc.(mg/ml)	*E.coli*	*K.pneumoniae*	*B.subtilis*	*S.aureus*
Co_3O_4(1:1)	50, 75, and 100	1.5,6,6	6,21,16	6,6,6	6,6,6
Co_3O_4(1:2)	50, 75, and 100	17,13,6	6,6,6	10,6,0.9	6,6,6
Co_3O_4(2:1)	50, 75, and 100	11, 6,6	6,6,6	6,6,6	6,6,6
ZnO(1:1)	50, 75, and 100	6,6,6	6,6,6	6,6,6	6,6,6
ZnO (1:2)	50, 75, and 100	7,9,11	6,6,6	6, 10,15	6,6,6
ZnO(2:1)	50, 75, and 100	12,0.7,8	6,6,6	6,6,6	6,6,6
Co_3O_4-ZnO(1:1)	50, 75, and 100	6,6,6	6,6,6	8,6,6	10, 12,6
Co_3O_4-ZnO(1:2)	50, 75, and 100	6,12,7	6,6,6	6,6,6	12,15,17
Co_3O_4-ZnO(2:1)	50, 75, and 100	6,6,6	6,6,6	6,6,6	6,6,6
Erythromycin(+ve) control		28	28	24	24

5. CONCLUSION AND RECOMMENDATION

5.1. Conclusion

In this study, Co_3O_4**,** ZnO NPs, and Co_3O_4-ZnO nanocomposites were synthesized by a green sol gel method using extract of potato and banan peels as capping agent. More crystalline nature and best performing Co_3O_4**,** ZnO NPs, and Co_3O_4-ZnO nanocomposites were obtained when it was biosynthesized within a 1:2 ratio. The particles were found to be thermally stable above 400℃. Structural studies revealed that synthesized Co_3O_4-ZnO nanocomposites were found with purely spinel-type Co_3O_4 and hexagonal wurtzite ZnO. SEM reveals the morphology as spherical. Optical studies have showed the shift in absorption wavelength towards higher wavelength that confirms formation of Co_3O_4-ZnO hetero-junction and the bandgap narrowing with enhancement in the visible light absorption. Functional group analysis indicates the presence of various capping and stabilizing agents.

The antibacterial activity of the biosynthesized three ratios of Co_3O_4**,** ZnO NPs, and Co_3O_4-ZnO nanocomposites using extract of potato and banana peels were investigated. Among the different ratios of Co_3O_4**,** ZnO NPs, and Co_3O_4-ZnO nanocomposites (1:2) have better performing antibacterial activity. More over the extract of potato peel stabilized ZnO NPs exhibited considerable than Co_3O_4 NPs and Co_3O_4-ZnO nanocomposites antimicrobial activity against pathogenic bacteria. Based on these we conclude that the extract of fruit peel stabilized ZnO NPs have potential biomedical applications when compared to synthesized Co_3O_4 NPs and Co_3O_4-ZnO nanocomposite peel due to its enhanced stability and small size.

5.2. Recommendations

For the future study, there are a few recommendations on the characterization of Co_3O_4-ZnO nanocomposites that will give full information. The elemental distribution and chemical composition of the synthesized samples should be characterized by energy depressive X-ray (EDX) and X-ray photoelectron spectroscopy (XPS). In order to investigate the particle size, more detail morphology and surface area of nanocomposite the samples should be characterized by TEM and BET instruments respectively.

6. REFERENCE

1. DeSimone, J.M., *Practical approaches to green solvents.* Science, 2002. **297**(5582): p. 799-803.
2. Rana, S. and P. Kalaichelvan, *Ecotoxicity of nanoparticles.* ISRN toxicology, 2013. **2013**.
3. Kitakami, O., et al., *Size effect on the crystal phase of cobalt fine particles.* Physical Review B, 1997. **56**(21): p. 13849.
4. Jahan, M., M. Warsi, and F. Khatoon, *Concentration influence on antimicrobial activity of banana blossom extract-incorporated chitosan-polyethylene glycol (CS-PEG) blended film.* J Chem Pharm Res, 2010. **2**(5): p. 373-378.
5. Wuyts, N., D. De Waele, and R. Swennen, *Extraction and partial characterization of polyphenol oxidase from banana (Musa acuminata Grande naine) roots.* Plant physiology and biochemistry, 2006. **44**(5-6): p. 308-314.
6. Daniells, S., *Banana skin could offer cheap pectin from waste.* Dry tech, 2000. **18**: p. 1327-7.
7. Ighodaroro, O., J. Mairiga, and A. Adeyi, *Reducing and anti-proxidant profiles of flavonoids in Ocimum gratissimum.* Int J. Chem. Science, 2009. **2**: p. 85-89.
8. Fagbemi, J.F., et al., *Evaluation of the antimicrobial properties of unripe banana (Musa sapientum L.), lemon grass (Cymbopogon citratus S.) and turmeric (Curcuma longa L.) on pathogens.* African Journal of Biotechnology, 2009. **8**(7).
9. Levy, S.B. and B. Marshall, *Antibacterial resistance worldwide: causes, challenges and responses.* Nature medicine, 2004. **10**(12): p. S122-S129.
10. Mandal, S., et al., *Antibacterial activity of ciprofloxacin and trimethoprim, alone and in combination, against Vibrio cholerae O 1 Biotype El Tor serotype Ogawa isolates.* Polish journal of microbiology, 2009. **58**(1): p. 57-60.
11. Mah, T.-F.C. and G.A. O'Toole, *Mechanisms of biofilm resistance to antimicrobial agents.* Trends in microbiology, 2001. **9**(1): p. 34-39.
12. Saga, T. and K. Yamaguchi, *History of antimicrobial agents and resistant bacteria.* Jmaj, 2009. **52**(2): p. 103-108.

13. Mandal, S., et al., *Synergistic anti–Staphylococcus aureus activity of amoxicillin in combination with Emblica officinalis and Nymphae odorata extracts.* Asian Pacific Journal of Tropical Medicine, 2010. **3**(9): p. 711-714.
14. Basualdo, C., et al., *Comparison of the antibacterial activity of honey from different provenance against bacteria usually isolated from skin wounds.* Veterinary microbiology, 2007. **124**(3-4): p. 375-381.
15. Friedman, M., et al., *Anticarcinogenic effects of glycoalkaloids from potatoes against human cervical, liver, lymphoma, and stomach cancer cells.* Journal of agricultural and food chemistry, 2005. **53**(15): p. 6162-6169.
16. Schieber, A. and M.D. Saldaña, *Potato peels: a source of nutritionally and pharmacologically interesting compounds-a review.* 2009.
17. Sekhon, B.S., *Metalloantibiotics and antibiotic mimics-an overview.* Journal of Pharmaceutical Education and Research, 2010. **1**(1): p. 1.
18. Padmavathy, N. and R. Vijayaraghavan, *Enhanced bioactivity of ZnO nanoparticles—an antimicrobial study.* Science and technology of advanced materials, 2008. **9**(3): p. 035004.
19. Özgür, Ü., et al., *A comprehensive review of ZnO materials and devices.* Journal of applied physics, 2005. **98**(4): p. 11.
20. Ristić, M., et al., *Sol–gel synthesis and characterization of nanocrystalline ZnO powders.* Journal of Alloys and Compounds, 2005. **397**(1-2): p. L1-L4.
21. Wu, C., et al., *A novel chemical route to prepare ZnO nanoparticles.* Materials Letters, 2006. **60**(15): p. 1828-1832.
22. Hu, X.-L., Y.-J. Zhu, and S.-W. Wang, *Sonochemical and microwave-assisted synthesis of linked single-crystalline ZnO rods.* Materials Chemistry and physics, 2004. **88**(2-3): p. 421-426.
23. Wang, G., et al., *Large-scale synthesis of aligned hexagonal ZnO nanorods using chemical vapor deposition.* Materials Letters, 2004. **58**(16): p. 2195-2198.
24. Liu, Y., Z. Liu, and G. Wang, *Synthesis and characterization of ZnO nanorods.* Journal of crystal growth, 2003. **252**(1-3): p. 213-218.

25. Owens, G.J., et al., *Sol–gel based materials for biomedical applications.* Progress in Materials Science, 2016. **77**: p. 1-79.
26. Liao, J.-Y., et al., *Tri-functional hierarchical TiO_2 spheres consisting of anatase nanorods and nanoparticles for high efficiency dye-sensitized solar cells.* Energy & Environmental Science, 2011. **4**(10): p. 4079-4085.
27. Matthews, L., et al., *Applications of nanomedicine in antibacterial medical therapeutics and diagnostics.* Open tropical medicine journal, 2010. **3**(1): p. 1-9.
28. Issa, B., et al., *Magnetic nanoparticles: surface effects and properties related to biomedicine applications.* International journal of molecular sciences, 2013. **14**(11): p. 21266-21305.
29. Li, X.-q. and W.-x. Zhang, *Iron nanoparticles: The core− shell structure and unique properties for Ni (II) sequestration.* Langmuir, 2006. **22**(10): p. 4638-4642.
30. Li, Y., et al., *Nanocrystalline silver particles: synthesis, agglomeration, and sputtering induced by electron beam.* Journal of colloid and interface science, 1999. **209**(2): p. 347-349.
31. Sorbiun, M., et al., *Biosynthesis of metallic nanoparticles using plant extracts and evaluation of their antibacterial properties.* Nanochemistry Research, 2018. **3**(1): p. 1-16.
32. Ankamwar, B., M. Chaudhary, and M. Sastry, *Gold nanotriangles biologically synthesized using tamarind leaf extract and potential application in vapor sensing.* Synthesis and Reactivity in Inorganic, Metal-Organic and Nano-Metal Chemistry, 2005. **35**(1): p. 19-26.
33. Ledwith, D.M., A.M. Whelan, and J.M. Kelly, *A rapid, straight-forward method for controlling the morphology of stable silver nanoparticles.* Journal of Materials Chemistry, 2007. **17**(23): p. 2459-2464.
34. Morones, J.R., et al., *The bactericidal effect of silver nanoparticles.* Nanotechnology, 2005. **16**(10): p. 2346.
35. Löffler, J.F., et al., *Crossover in the magnetic properties of nanostructured metals.* Materials Science and Engineering: A, 2001. **304**: p. 1050-1054.

36. Zhang, Y., et al., *Microstructure and magnetic behavior of carbon-coated Co nanoparticles studied by nuclear magnetic resonance.* Applied Physics Letters, 2000. **76**(1): p. 94-96.
37. Yu, M., et al., *Flower-like carbonyl iron powder modified by nanoflakes: Preparation and microwave absorption properties.* Applied Physics Letters, 2015. **106**(16): p. 161904.
38. Wang, C., et al., *Antibacterial effects of zinc oxide nanoparticles on Escherichia coli K88.* African Journal of Biotechnology, 2012. **11**(44): p. 10248-10254.
39. Banoee, M., et al., *ZnO nanoparticles enhanced antibacterial activity of ciprofloxacin against Staphylococcus aureus and Escherichia coli.* Journal of Biomedical Materials Research Part B: Applied Biomaterials, 2010. **93**(2): p. 557-561.
40. Jalal, R., M. Saliani, and E. Goharshadi. *Effects of pH and concentration on antibacterial activity of ZnO nanofluids against Staphylococcus aureus*. in *1st National Iranian New Chemistry Congress*. 2011.
41. Meruvu, H., et al., *Synthesis and characterization of zinc oxide nanoparticles and its antimicrobial activity against Bacillus subtilis and Escherichia coli.* J. Rasayan Chem, 2011. **4**(1): p. 217-222.
42. Jones, N., et al., *Antibacterial activity of ZnO nanoparticle suspensions on a broad spectrum of microorganisms.* FEMS microbiology letters, 2008. **279**(1): p. 71-76.
43. Salavati-Niasari, M., N. Mir, and F. Davar, *Synthesis and characterization of Co_3O_4 nanorods by thermal decomposition of cobalt oxalate.* Journal of Physics and Chemistry of Solids, 2009. **70**(5): p. 847-852.
44. Kim, H., et al., *Exceptional lithium storage in a $Co(OH)_2$ anode: hydride formation.* ACS nano, 2018. **12**(3): p. 2909-2921.
45. Barsan, N., D. Koziej, and U. Weimar, *Metal oxide-based gas sensor research: How to?* Sensors and Actuators B: Chemical, 2007. **121**(1): p. 18-35.
46. Barman, J. and K. Sarma, *Structural and optical properties of CdS nanoparticles.* Indian Journal of Physics, 2008. **81**: p. 855-862.

47. Barua, S., et al., *Silver nanoparticles as antibacterial and anticancer materials against human breast, cervical and oral cancer cells.* Journal of nanoscience and nanotechnology, 2017. **17**(2): p. 968-976.
48. Borah, J., J. Barman, and K. Sarma, *Effect of pH on ZnS nanocrystalline thin film embedded in a polyvinyl alcohol matrix.* International Journal of modern physics B, 2010. **24**(29): p. 5663-5673.
49. Organization, W.H., *Guidelines for drinking-water quality*. 1993: World Health Organization.
50. Operations, U.S.E.P.A.O.o.W.P., *Alternative disinfectants and oxidants guidance manual*. 1999: US Environmental Protection Agency, Office of Water.
51. Siraj, K.T. and P.P. Rao, *Review on current world water resources scenario and water treatment technologies and techniques.* IJAR, 2016. **2**(4): p. 262-266.
52. Biradar, D., K. Lingappa, and A. Dayanand, *Antibacterial activity of nano goldparticles synthesized by Bacillus Sps.* Journal of Ecobiotechnology, 2012.
53. Ahmed, S., et al., *Green synthesis of silver nanoparticles using Azadirachta indica aqueous leaf extract.* Journal of Radiation Research and Applied Sciences, 2016. **9**(1): p. 1-7.
54. Yarestani, M., et al., *Hydrothermal synthesis of cobalt oxide nanoparticles: Its optical and magnetic properties.* Journal of Sciences, Islamic Republic of Iran, 2014. **25**(4): p. 339-343.
55. Mukherjee, P., et al., *Fungus-mediated synthesis of silver nanoparticles and their immobilization in the mycelial matrix: a novel biological approach to nanoparticle synthesis.* Nano Letters, 2001. **1**(10): p. 515-519.
56. Seabra, A.B. and N. Durán, *Nanotoxicology of metal oxide nanoparticles.* Metals, 2015. **5**(2): p. 934-975.
57. Jun, Y.W., J.H. Lee, and J. Cheon, *Chemical design of nanoparticle probes for high-performance magnetic resonance imaging.* Angewandte Chemie International Edition, 2008. **47**(28): p. 5122-5135.
58. Lu, P., et al., *Abnormal room temperature ferromagnetism in CuO/ZnO nanocomposites via hydrothermal method.* Applied Surface Science, 2017. **399**: p. 396-402.

59. Das, S. and V.C. Srivastava, *Synthesis and characterization of ZnO/CuO nanocomposite by electrochemical method.* materials science in semiconductor processing, 2017. **57**: p. 173-177.
60. Kaviyarasu, K., et al., *Synthesis and characterization studies of MgO: CuO nanocrystals by wet-chemical method.* Spectrochimica Acta Part A: Molecular and Biomolecular Spectroscopy, 2015. **142**: p. 405-409.
61. Hassanpour, M., et al., *Nano-sized CuO/ZnO hollow spheres: synthesis, characterization and photocatalytic performance.* Journal of Materials Science: Materials in Electronics, 2017. **28**(19): p. 14678-14684.
62. Gajendiran, J. and V. Rajendran, *Synthesis and characterization of coupled semiconductor metal oxide (ZnO/CuO) nanocomposite.* Materials Letters, 2014. **116**: p. 311-313.
63. Udayabhaskar, R. and B. Karthikeyan, *Optical and phonon properties of ZnO: CuO mixed nanocomposite.* Journal of Applied Physics, 2014. **115**(15): p. 154303.
64. Sathishkumar, P., et al., *Synthesis of CuO-ZnO nanophotocatalyst for visible light assisted degradation of a textile dye in aqueous solution.* Chemical Engineering Journal, 2011. **171**(1): p. 136-140.
65. Saravanan, R., et al., *Enhanced photocatalytic activity of ZnO/CuO nanocomposite for the degradation of textile dye on visible light illumination.* Materials Science and Engineering: C, 2013. **33**(1): p. 91-98.
66. Souli, M., et al., *Antimicrobial activity of copper surfaces against carbapenemase-producing contemporary Gram-negative clinical isolates.* Journal of Antimicrobial Chemotherapy, 2013. **68**(4): p. 852-857.
67. Rai, M.K., et al., *Silver nanoparticles: the powerful nanoweapon against multidrug-resistant bacteria.* Journal of applied microbiology, 2012. **112**(5): p. 841-852.
68. Li, Q., et al., *Epidemiology of human infections with avian influenza A (H7N9) virus in China.* New England Journal of Medicine, 2014. **370**(6): p. 520-532.
69. REZAEI, Z.S., et al., *Comparative study of antimicrobial activities of TiO2 and CdO nanoparticles against the pathogenic strain of Escherichia coli.* 2010.

70. Henderson, D.K., *Managing methicillin-resistant staphylococci: a paradigm for preventing nosocomial transmission of resistant organisms.* The American journal of medicine, 2006. **119**(6): p. S45-S52.
71. Ansari, M., H. Khan, and A. Khan, *Evaluation of antibacterial activity of silver nanoparticles against MSSA and MSRA on isolates from skin infections.* 2011.
72. Ravishankar Rai, V., *Nanoparticles and their potential application as antimicrobials.* 2011.
73. Dwivedi, S., et al., *Reactive oxygen species mediated bacterial biofilm inhibition via zinc oxide nanoparticles and their statistical determination.* PloS one, 2014. **9**(11): p. e111289.
74. Bishop, G.M., R. Dringen, and S.R. Robinson, *Zinc stimulates the production of toxic reactive oxygen species (ROS) and inhibits glutathione reductase in astrocytes.* Free Radical Biology and Medicine, 2007. **42**(8): p. 1222-1230.
75. Kumar, R., et al., *Antimicrobial properties of ZnO nanomaterials: A review*. Ceramics International, 2017. **43**(5): p. 3940-3961.
76. Mishra, P.K., et al., *Zinc oxide nanoparticles: a promising nanomaterial for biomedical applications.* Drug discovery today, 2017. **22**(12): p. 1825-1834.
77. Al, A.Q.A.E.-k. and H. Qassem, *Synthesis of Metallic/Metallic Oxide Nanoparticles in Surfactant Shell and Investigating their Anti-bacterial Activities*. 2013.
78. Harris, L.G., S. Foster, and R.G. Richards, *An introduction to Staphylococcus aureus, and techniques for identifying and quantifying S. aureus adhesins in relation to adhesion to biomaterials: review.* Eur Cell Mater, 2002. **4**(3): p. 100-20.
79. Altaee, N., M.J. Kadhim, and I.H. Hameed, *Characterization of metabolites produced by E. coli and analysis of its chemical compounds using GC-MS.* International Journal of Current Pharmaceutical Review and Research, 2017. **7**(6): p. 13-19.
80. Podschun, R. and U. Ullmann, *Klebsiella spp. as nosocomial pathogens: epidemiology, taxonomy, typing methods, and pathogenicity factors.* Clinical microbiology reviews, 1998. **11**(4): p. 589-603.
81. Giske, C.G., et al., *Clinical and economic impact of common multidrug-resistant gram-negative bacilli.* Antimicrobial agents and chemotherapy, 2008. **52**(3): p. 813-821.

82. Muniappan, R., G.V. Reddy, and A. Raman, *Biological control of tropical weeds using arthropods*. 2009: Cambridge University Press.

83. Sone, B., et al., *Sm_2O_3 nanoparticles green synthesis via Callistemon viminalis' extract.* Journal of Alloys and Compounds, 2015. **650**: p. 357-362.

84. Bamisaye, F., et al., *Medico-botanical investigation of siam weed (chromolaena odorata) used among the "ijebu" people of Ogun state, Nigeria.* J Med Med Sci, 2014. **5**(1): p. 20-4.

85. Hafeez, M., et al., *Populus ciliata leaves extract mediated synthesis of zinc oxide nanoparticles and investigation of their anti-bacterial activities.* Materials Research Express, 2019. **6**(7): p. 075064.

86. Samanta, P., et al., *Visible emission from ZnO nanorods synthesized by a simple wet chemical method.* Int. J. Nanosci. Nanotechnol, 2009. **1**(1-2): p. 81-90.

87. Hu, J., et al., *Synthesis and characterization of Cobalt-doped ZnO microstructures for methane gas sensing.* Applied Surface Science, 2016. **363**: p. 181-188.

88. Giahi, M., et al., *Synthesis of CuO/ZnO nanoparticles and their application for photocatalytic degradation of lidocaine HCl by the trial-and-error and Taguchi methods.* Bulletin of the Korean Chemical Society, 2013. **34**(7): p. 2176-2182.

89. Huang, Y., et al., *Synthesis of cobalt based complexes and conversion to Co_3O_4 nanoparticles as a high performance anode for lithium ion battery.* Electrochimica Acta, 2014. **145**: p. 34-39.

90. Ahmad, T., et al., *Nanorods of transition metal oxalates: A versatile route to the oxide nanoparticles.* Arabian Journal of Chemistry, 2011. **4**(2): p. 125-134.

91. Palacios-Hernández, T., et al., *Synthesis of Cu and Co metal oxide nanoparticles from thermal decomposition of tartrate complexes.* Inorganica Chimica Acta, 2012. **392**: p. 277-282.

92. Sharma, G. and P. Jeevanandam, *Synthesis of MgO supported Co_3O_4 nanoparticles by a novel thermal decomposition approach and studies on their magnetic properties.* Microporous and mesoporous materials, 2013. **165**: p. 55-62.

93. Xu, J., et al., *Synthesis and photoluminescence of well-dispersible anatase TiO_2 nanoparticles.* Journal of Colloid and Interface Science, 2008. **318**(1): p. 29-34.

94. Pookmanee, P. and S. Phanichphant, *Titanium dioxide powder prepared by a sol-gel method.* Journal of Ceramic Processing Research, 2009. **10**(2): p. 167-170.
95. López, A., et al., *Nanostructured low crystallized titanium dioxide thin films with good photocatalytic activity.* Powder Technology, 2010. **202**(1-3): p. 111-117.
96. Vijayalakshmi, R. and V. Rajendran, *Synthesis and characterization of nano-TiO_2 via different methods.* Archives of Applied Science Research, 2012. **4**(2): p. 1183-1190.
97. Herrera, M., et al., *In vitro antibacterial activity of glass-ionomer cements.* Microbios, 2001. **104**(409): p. 141.
98. Igwe, O. and E. Ekebo, *Biofabrication of cobalt nanoparticl odorata and their potentia.* Res. J. Chem. Sci., 2018. **1**: p. 11-17.
99. Cuscó, R., et al., *Temperature dependence of Raman scattering in ZnO.* Physical Review B, 2007. **75**(16): p. 165202.
100. Abraham, N., et al., *Dye sensitized solar cells using catalytically active CuO-ZnO nanocomposite synthesized by single step method.* Spectrochimica Acta Part A: Molecular and Biomolecular Spectroscopy, 2018. **200**: p. 116-126.
101. Hezam, A., et al., *Heterogeneous growth mechanism of ZnO nanostructures and the effects of their morphology on optical and photocatalytic properties.* CrystEngComm, 2017. **19**(24): p. 3299-3312.
102. Zhang, L., et al., *Facile synthesis of mesoporous ZnO/ Co_3O_4 microspheres with enhanced gas-sensing for ethanol.* Sensors and Actuators B: Chemical, 2015. **221**: p. 1492-1498.
103. Athar, T., et al., *Wet synthesis of monodisperse cobalt oxide nanoparticles.* ISRN materials science, 2012. **2012**.
104. Khan, S.H., B. Pathak, and M. Fulekar. *Development of zinc oxide nanoparticle by sonochemical method and study of their physical and optical properties*. in *AIP Conference Proceedings*. 2016. AIP Publishing LLC.
105. He, T., et al., *Solubility-controlled synthesis of high-quality Co_3O_4 nanocrystals.* Chemistry of materials, 2005. **17**(15): p. 4023-4030.

106. Divya, M., et al., *Synthesis of zinc oxide nanoparticle from Hibiscus rosa-sinensis leaf extract and investigation of its antimicrobial activity.* Res. J. Pharm. Biol. Chem, 2013. **4**(2): p. 1137-1142.
107. Prabhu, Y., et al., *Surfactant assisted synthesis of ZnO nanoparticles, characterization and its antimicrobial activity against Staphylococcus aureus and Escherichia coli.* Int J Curr Eng Technol, 2014. **4**: p. 1038-1041.
108. Nagarajan, S. and K.A. Kuppusamy, *Extracellular synthesis of zinc oxide nanoparticle using seaweeds of gulf of Mannar, India.* Journal of nanobiotechnology, 2013. **11**(1): p. 39.
109. Kundu, D., et al., *Extracellular biosynthesis of zinc oxide nanoparticles using Rhodococcus pyridinivorans NT2: multifunctional textile finishing, biosafety evaluation and in vitro drug delivery in colon carcinoma.* Journal of photochemistry and photobiology B: Biology, 2014. **140**: p. 194-204.
110. Kandjani, A.E., et al., *Optical and magnetic properties of Co_3O_4/ZnO core/shell nanoparticles.* Journal of optoelectronics and advanced materials, 2010. **12**(10): p. 2057-2062.
111. Wang, X., et al., *One-dimensional arrays of Co_3O_4 nanoparticles: synthesis, characterization, and optical and electrochemical properties.* The Journal of Physical Chemistry B, 2004. **108**(42): p. 16401-16404.
112. Xu, R. and H.C. Zeng, *Self-generation of tiered surfactant superstructures for one-pot synthesis of Co_3O_4 nanocubes and their close-and non-close-packed organizations.* Langmuir, 2004. **20**(22): p. 9780-9790.
113. Chitra, K. and G. Annadurai, *Antimicrobial activity of wet chemically engineered spherical shaped ZnO nanoparticles on food borne pathogen.* International food research journal, 2013. **20**(1).
114. Emaga, T.H., et al., *Effects of the stage of maturation and varieties on the chemical composition of banana and plantain peels.* Food chemistry, 2007. **103**(2): p. 590-600.
115. Albishi, T., et al., *Phenolic content and antioxidant activities of selected potato varieties and their processing by-products.* Journal of Functional Foods, 2013. **5**(2): p. 590-600.

116. Farhadi, S., J. Safabakhsh, and P. Zaringhadam, *Synthesis, characterization, and investigation of optical and magnetic properties of cobalt oxide (Co_3O_4) nanoparticles.* Journal of Nanostructure in Chemistry, 2013. **3**(1): p. 69.
117. Makhlouf, M.T., B. Abu-Zied, and T. Mansoure, *Direct fabrication of cobalt oxide nano-particles employing glycine as a combustion fuel.* Physical Chemistry, 2012. **2**(6): p. 86-93.
118. Teng, Y., et al., *One-pot hydrothermal synthesis of uniformly cubic Co_3O_4 nanocrystals.* Materials Letters, 2010. **64**(3): p. 239-242.
119. Lakshmeesha, T., et al., *Reactivity of crystalline ZnO superstructures against fungi and bacterial pathogens: synthesized using Nerium oleander leaf extract.* Crystal growth & design, 2014. **14**(8): p. 4068-4079.
120. Li, B. and Y. Wang, *Facile synthesis and photocatalytic activity of ZnO–CuO nanocomposite.* Superlattices and Microstructures, 2010. **47**(5): p. 615-623.
121. Li, X., et al., *Antibacterial and physical properties of poly (vinyl chloride)-based film coated with ZnO nanoparticles.* Food Science and Technology International, 2010. **16**(3): p. 225-232.
122. Sirelkhatim, A., et al., *Review on zinc oxide nanoparticles: antibacterial activity and toxicity mechanism.* Nano-micro letters, 2015. **7**(3): p. 219-242.